Generalization of Pareto-Optimality for Many-Objective Evolutionary Optimization

Chenwen Zhu, Lihong Xu, *Member, IEEE*, and Erik D. Goodman

***Abstract*—The vast majority of multiobjective evolutionary algorithms presented to date are Pareto-based. Usually, these algorithms perform well for problems with few (two or three) objectives. However, due to the poor discriminability of Pareto-optimality in many-objective spaces (typically four or more objectives), their effectiveness deteriorates progressively as the problem dimension increases. This paper generalizes Pareto-optimality both symmetrically and asymmetrically by expanding the dominance area of solutions to enhance the scalability of existing Pareto-based algorithms. The generalized Pareto-optimality (GPO) criteria are comparatively studied in terms of the distribution of ranks, the ranking landscape, and the convergence of the evolutionary process over several benchmark problems. The results indicate that algorithms equipped with a generalized optimality criterion can acquire the flexibility of changing their selection pressure within certain ranges, and achieve a richer variety of ranks to attain faster and better convergence on some subsets of the Pareto optima. To compensate for the possible diversity loss induced by the generalization, a distributed evolution framework with adaptive parameter setting is also proposed and briefly discussed. Empirical results indicate that this strategy is quite promising in diversity preservation for algorithms associated with the GPO.**

***Index Terms*—Computational intelligence, evolutionary algorithms (EAs), generalized Pareto-optimality (GPO), genetic algorithms, multiobjective optimization.**

I. INTRODUCTION

MANY real-world optimization problems involve multiple conflicting objectives that must be considered simultaneously. Without sufficient preference information, the presence of these conflicting objectives inexorably entails the impossibility of finding a single solution that is globally optimal in terms of all the objectives. In such a case, instead of a total order, only partial orders between different solutions can be expected, resulting in a solution set consisting of a suite of differently compromised alternatives. However, one of the predicaments in the multiobjective context is that there does not exist a unique or straightforward (compared with single objective optimization) quality assessment method to classify all the solutions obtained and to guide the following search (if any) for better ones.

Evolutionary algorithms (EAs), which deal simultaneously with a set of possible solutions, seem particularly suitable for addressing multiobjective optimization problems (MOPs) and have been studied intensively for many years (see [1], [2], and references therein). To solve the aforementioned predicament, the concept of Pareto dominance, an intuitive yet qualitative notion of compromise, is commonly adopted to rank solutions by the vast majority of multiobjective EAs (MOEAs) presented to date—examples of these MOEAs are the nondominated sorting genetic algorithm II (NSGA-II) [3], the strength Pareto EA 2 [4], and so on [5]–[12]. When the dimensionality of the problem at hand is small (i.e., two or three), as is usually the case in the literature, the performance of most contemporary Pareto-based MOEAs can be quite good. But when it comes to high dimensions (i.e., four or more), the effectiveness of these algorithms deteriorate dramatically as the number of objectives increases, which has already been both theoretically attested [13]–[15] and experimentally evidenced [16]–[19].

For many-objective optimization problems (MaOPs), the performance degradation, coming along with the dimensionality increase, of Pareto-based MOEAs mainly results from two factors. First, the solution sparsity, rooted in the notorious but inevitable "curse of dimensionality," not only raises a quantitative burden on solutions, but also weakens the recombination operators, and complicates the diversity preservation [20]. Second, the solution discriminability of Pareto dominance, or the resultant selection pressure, is susceptible to dimensionality—namely, the proportion of qualitatively indistinguishable solutions in a population increases so rapidly with the number of objectives that the selection procedure in this situation is carried out almost at random or guided merely by diversity criteria [21]. It is also worth noting that even if the first issue can be somehow addressed, the scalability problem remains, which implies that the second issue is the predominant one to which the poor dimensional scalability of Pareto-based MOEAs should be attributed.

To alleviate the intractability of a many-dimensional space for Pareto-based MOEAs, one can either cut it explicitly

Manuscript received November 16, 2014; revised March 12, 2015, May 19, 2015, and June 22, 2015; accepted July 12, 2015. Date of publication July 15, 2015; date of current version March 29, 2016. This work was supported in part by the National High Technology Research and Development Program (863 Programs) of China under Grant 2012AA10A507, in part by the National Natural Science Foundation of China under Grant 61174090 and Grant 61374094, and in part by the U.S. National Science Foundation's Bio/computational Evolution in Action Consortium Center for the Study of Evolution in Action under Cooperative Agreement DBI-0930454. *(Corresponding author: Lihong Xu.)*

C. Zhu and L. Xu are with the College of Electronics and Information Engineering, Tongji University, Shanghai 201804, China (e-mail: zhchwn@gmail.com; xulhk@163.com).

E. D. Goodman is with Bio/computational Evolution in Action Consortium Center for the Study of Evolution in Action, Michigan State University, East Lansing, MI 48823 USA (e-mail: goodman@egr.msu.edu).

Color versions of one or more of the figures in this paper are available online at http://ieeexplore.ieee.org.

Digital Object Identifier 10.1109/TEVC.2015.2457245

(e.g., confining the problem to a minimal subset of conflicting objectives [22], [23], decomposing the problem into several subproblems [24]–[26]) or decrease it implicitly (e.g., exploiting only regions of interest by incorporating decision-makers' preferences [27]–[29], or guide the search process by setting multiple targets [30]–[32]). Though highly effective for some specific instances, lowering the difficulty of many-objective problems through such means is still only a partial circumvention of the failure of Pareto dominance, as the possibility of occurrence of dominance-resistant solutions [33] (i.e., solutions with extremely poor values in at least one of the objectives, but with near optimal values in the others) still exists. Therefore, introducing alternative optimality criteria which can provide better solution discriminability than Pareto-optimality seems worth investigating as a remedy for evolutionary many-objective optimization. In fact, many studies have addressed this issue in various ways. A straightforward idea is to modify the Pareto dominance relation to enhance Pareto-based MOEAs' selection pressure, e.g., dominance area controlling [34]–[37], guided dominance [38], k-optimality [21], α-dominance [33], subspace dominance comparison [39], [40], preference ordering [41], [42], cone dominance [43], and fuzzy Pareto dominance [44]. Another avenue to augment the selection process is to design some non-Pareto-based dominance ranking techniques, e.g., average rank [45], maximum rank [46], ranking dominance [47], favor relation [48], [49], winning score relation [50], and distance-based ranking [51]–[53]. In addition, some selection criteria that naturally integrate proximity and diversity of solutions have also been developed, including aggregation-based criteria (e.g., single objective Pareto sampling [54] and directed line search [55]), indicator-based criteria (e.g., hypervolume estimation [56], [57], and dominated hypervolume [58]), and gridding-based criteria (e.g., ε-dominance [59], cone ε-dominance [60], and grid dominance [61]). Despite the risk of leading the final solution set to some subareas of the Pareto-optimal front [13], [62], these alternative optimality criteria, especially the relaxed forms of Pareto dominance, have been found to be promising in converging toward the global optimum.

Although a variety of alternative optimality criteria accommodating MOEAs to many-objective optimization have been proposed, their usage is largely restricted by one or more of the following drawbacks.

1) *Diversity Loss:* Different optimality criteria have different solution biases—some prefer extreme solutions while some others prefer the best-compromised ones, as defined by themselves. Consequently, solution diversity is difficult to maintain and only part of the Pareto-optimal front will be reliably found.
2) *High Computational Cost:* The calculation (or estimation) of some optimality criteria needs to repeatedly traverse the whole objective space and even all of its subspaces, which makes the computational burden of the corresponding MOEAs grow exponentially as the problem dimensionality increases.
3) *Conflicts of Dominance Relation:* Two solutions might dominate each other if their dominating spaces are modified inappropriately. In this case, the expected inferior-to-superior relationship of solutions is broken, and the survivability of a solution will depend not only on its objective values, but also on its order in the population.
4) *Parameter Selection Difficulty:* The scalability of some optimality criteria is ensured by their flexible parameter settings. However, it is usually difficult, or even impossible, to determine the quantitative relationship between the solution discriminability of an optimality criterion and a given set of its parameters.

Therefore, some improvements are still needed before MOEAs can be considered as an effective optimizer for MaOPs as for problems with fewer—i.e., two or three—objectives.

In view of this dilemma, this paper proposes a generalized Pareto-optimality (GPO) to tackle the scalability problem of Pareto-based MOEAs. The basic idea of GPO is to progressively expand the dominance area of solutions as the problem dimensionality increases, thereby maintaining a relatively consistent level of solution discriminability across a range of many objectives. As a generalized form of the conventional Pareto-optimality (CPO), GPO is designed to be totally compatible with CPO without introducing much extra computational complexity. The only parameter that needs to be fixed in GPO is the expanding angle which controls the expansion degree of the dominance area, and it can be easily configured with the aid of the parameter setting guidelines provided—i.e., a "pseudo-2-D" principle and an adaptive chopping principle. This paper is mainly inspired by a strategy called controlling-dominance-area-of-solutions (CDAS) [34] and the three major contributions are enumerated as the following.

1) A symmetric and an asymmetric generalization of CPO (AGPO) are accomplished to restrain the progressive loss of solution discriminability of Pareto dominance as the dimensionality of MOPs increases.
2) A systematic analysis of GPO is conducted both analytically and empirically to investigate its relative utility compared with some other optimality criteria.
3) A distributed MOEA framework based on the asymmetric GPO with adaptive parameter setting is suggested and briefly discussed as a means of compensating for the auxiliary diversity loss induced by the generalization of CPO.

The remainder of this paper is organized as described below. In Section II, some basic concepts of multiobjective optimization are presented. Section III describes the dominance-area-controlling technique and the motivation for modifying it. Section IV contains a symmetric and an AGPO along with some analyses of the resulting differences. Some static studies of GPO, including the parameter setting, the rank distribution, and the ranking landscape, are provided in Section V. Section VI dynamically compares GPO with some other optimality criteria based on several performance metrics. A distributed MOEA framework for diversity compensation is also proposed and briefly discussed in this section. Finally, Section VII reviews the main points of this paper and suggests some unexplored issues.

II. Multiobjective Optimization Concepts

Without loss of generality, a general MOP may be stated as a minimization problem of the following form [2].

Definition (MOP): Let $\mathbf{x}^* = [x_1^*, x_2^*, \ldots, x_N^*]^T$, find a solution set $\mathbf{P}^*(|\mathbf{P}^*| \geq 1)$ such that

$$\forall \mathbf{x}^* \in \mathbf{P}^* : \mathbf{x}^* = \arg\min_{\mathbf{x}\in\mathbf{D}} \mathbf{F}(\mathbf{x})$$
$$\text{s.t.} \begin{cases} \mathbf{G}(\mathbf{x}) \geq \mathbf{0} \\ \mathbf{H}(\mathbf{x}) = \mathbf{0} \end{cases} \tag{1}$$

where N is the dimension of the decision variable vector $\mathbf{x}$, which is bounded by $\mathbf{x}^L$ and $\mathbf{x}^U$. $\mathbf{D} \subset \mathbb{R}^N$ represents the decision space, i.e., $\mathbf{D} = [\mathbf{x}^L, \mathbf{x}^U]$. For constrained MOPs, K inequality constraints $\mathbf{G}(\mathbf{x}) = [g_1(\mathbf{x}), g_2(\mathbf{x}), \ldots, g_K(\mathbf{x})]^T$ and L equality constraints $\mathbf{H}(\mathbf{x}) = [h_1(\mathbf{x}), h_2(\mathbf{x}), \ldots, h_L(\mathbf{x})]^T$, which act on $\mathbf{D}$ to define a subset $\mathbf{\Omega}$ signifying the feasible region, must be satisfied. The function $\mathbf{F} : \mathbf{\Omega} \mapsto \mathbf{\Lambda} \subset \mathbb{R}^M$ is defined as the vector of the objective functions $\mathbf{F}(\mathbf{x}) = [f_1(\mathbf{x}), f_2(\mathbf{x}), \ldots, f_M(\mathbf{x})]^T$, and M and $\mathbf{\Lambda}$ are the dimensionality and the objective space of the MOPs, respectively. By definition, a MaOP is also a MOP, but with a relatively larger number of objectives—i.e., $M > 3$.

The notion of optimality most commonly adopted in MOPs is termed Pareto-optimality. The formal definition is provided in the following.

Definition (Pareto Dominance): A vector $\mathbf{u} = [u_1, u_2, \ldots, u_M]^T$ is said to dominate another vector $\mathbf{v} = [v_1, v_2, \ldots, v_M]^T$ (denoted by $\mathbf{u} \preceq \mathbf{v}$) if and only if $\mathbf{v}$ is no less than $\mathbf{u}$, that is

$$\mathbf{u} \preceq \mathbf{v} \Leftrightarrow \forall i \in \boldsymbol{\mathcal{M}}, u_i \leq v_i \wedge \exists j \in \boldsymbol{\mathcal{M}} : u_j < v_j \tag{2}$$

where $\boldsymbol{\mathcal{M}} = \{1, 2, \ldots, M\}$.

Definition (Pareto-Optimality): A solution $\mathbf{x} \in \mathbf{\Omega}$ is said to be Pareto-optimal with respect to $\mathbf{\Omega}$ if and only if there is no $\mathbf{x}' \in \mathbf{\Omega}$ for which $\mathbf{v} = [f_1(\mathbf{x}'), f_2(\mathbf{x}'), \ldots, f_M(\mathbf{x}')]^T$ dominates $\mathbf{u} = [f_1(\mathbf{x}), f_2(\mathbf{x}), \ldots, f_M(\mathbf{x})]^T$.

For a given MOP, this definition usually does not provide a single optimal solution, but a suite of them. When mapped into the objective space, the associated vectors of these solutions are termed nondominated (denoted by $\mathbf{u} \sim \mathbf{v}$), and they are all part of the Pareto front.

Definition (Pareto Front): For a given MOP $\mathbf{F}(\mathbf{x})$, the Pareto front is formally defined as

$$\mathcal{PF} := \left\{\mathbf{u} = \mathbf{F}(\mathbf{x}) | \mathbf{x} \in \mathbf{\Omega} \wedge \neg\exists \mathbf{x}' \in \mathbf{\Omega} : \mathbf{F}(\mathbf{x}') \preceq \mathbf{F}(\mathbf{x})\right\}. \tag{3}$$

For the sake of clarity, we restrict our reasoning to $\mathbf{\Lambda} = \mathbf{F}(\mathbf{\Omega})$, and unless otherwise specified, a solution hereinafter refers to a vector in $\mathbf{\Lambda}$, not its counterpart in $\mathbf{\Omega}$.

III. From CDAS to GPO

It may be generalized that the ineffectiveness of Pareto dominance in high-dimensional spaces is manifested in two major aspects, namely fewer ranks and denser fronts. These two aspects are not isolated as they both are related to the lack of the dominance rank variety. For richer ranks and sparser fronts, the solution partitioning process needs to be refined. One straightforward idea is to modify the dominance area of solutions for higher solution discriminability.

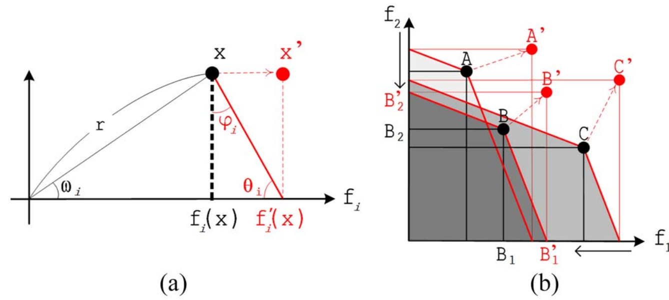

Fig. 1. (a) Demonstration of the fitness objective value transformation equation of CDAS in the ith dimension. (b) Application of CDAS to a 2-D problem.

As we know, Pareto dominance, by its definition, induces a partition onto the objective space. For any solution $\mathbf{u}$ within $\mathbf{\Lambda}$, its coordinates partition $\mathbf{\Lambda}$ into three subspaces in which other solutions having different dominance relations with $\mathbf{u}$ could lie. These subspaces (i.e., the dominating, dominated, and nondominated subspace) are, respectively, denoted by $\mathbf{\Lambda}_{\mathbf{u}}^{\preceq}$, $\mathbf{\Lambda}_{\mathbf{u}}^{\succeq}$, and $\mathbf{\Lambda}_{\mathbf{u}}^{\sim}$, and their relative sizes reflect the probabilities of the corresponding dominance relations solutions would have with the current solution $\mathbf{u}$. Take the nondominated subspace $\mathbf{\Lambda}_{\mathbf{u}}^{\sim}$ for example, for MOPs with two objectives, its relative size is 0.5, which means a solution has a probability of 50% to be nondominated with $\mathbf{u}$. However, this relative size increases with the problem dimensionality, and it impairs the selection process of MOEAs as more and more solutions become indistinguishable from the current one by dominance.

In view of this, CDAS controls (i.e., expands or contracts) the dominance area of solutions to regulate the selection pressure for Pareto-based MOEAs. As shown in Fig. 1(a), before the dominance relations among candidate solutions are calculated, the objective value of every solution in each dimension $f_i(\mathbf{x})$ is transformed to $f_i'(\mathbf{x})$ subject to a user-defined parameter $S \in [0.25, 0.75]$. The transformation equation for the ith objective of $\mathbf{F}(\mathbf{x})$ is given by

$$f_i'(\mathbf{x}) = \frac{r \cdot \sin(\omega_i + \theta_i)}{\sin(\theta_i)} \quad i \in \boldsymbol{\mathcal{M}} \tag{4}$$

where $r = \|\mathbf{F}(\mathbf{x})\|$, $\theta_i = S \cdot \pi$, and $f_i(\mathbf{x})$ and $f_i'(\mathbf{x})$ are the objective values in the ith dimension before and after the transformation, respectively. ω_i is the declination angle between $\mathbf{F}(\mathbf{x})$ and the direction vector of dimension i. This transformation is also illustrated in Fig. 1(b) for a 2-D case when $S < 0.5$. It is easy to see that the dominance areas of all solutions are expanded and finer grained ranking of given solutions is produced (e.g., the dominance relation between solutions B and C has been modified to $B \preceq C$ from $B \sim C$). Obviously, when $S = 0.5$, CDAS is just an exact equivalent of CPO since the dominance area of solutions remains unchanged.

In this paper, a concept called dominance envelope (DE) is introduced to describe the dominance area modification.

Definition (Dominance Envelope): For a given solution $\mathbf{u} = [u_1, u_2, \ldots, u_M]^T$ within $\mathbf{\Lambda} \subset \mathbb{R}^M$, the DE pertaining to $\mathbf{u}$ (denoted by $\mathcal{DE}_{\mathbf{u}}$) is the set of all solutions that are equal to

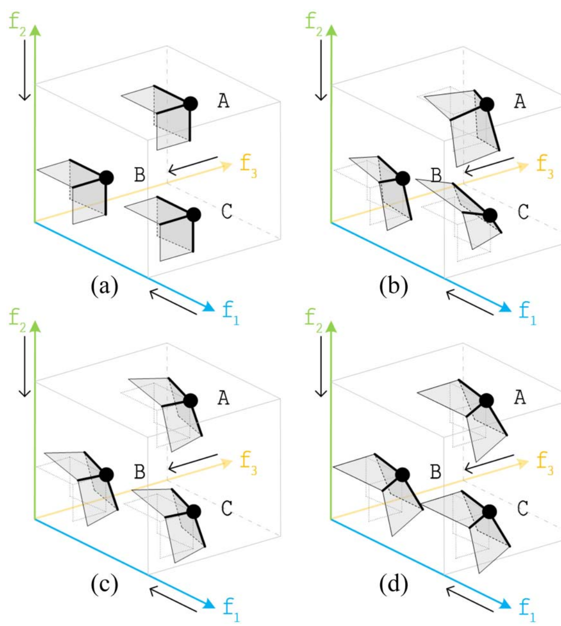

Fig. 2. Pictorial representation of partial DEs ($\mathbf{DE}^{\prec}$) produced by different optimality criteria in a 3-D objective space. (a) CPO. (b) CDAS. Prototype of (c) symmetric GPO and (d) asymmetric GPO. Obviously, only the DE in (b) varies solution by solution.

$\mathbf{u}$ in terms of at least 1-D—that is

$$\mathcal{DE}_{\mathbf{u}} := \{\mathbf{v} | \exists i \in \mathcal{M} : v_i = u_i\} \tag{5}$$

where $\mathbf{v} = [v_1, v_2, \ldots, v_M]^T$ is an arbitrary solution within $\mathbf{\Lambda}$. Clearly, $\mathcal{DE}_{\mathbf{u}}$ delimits the above-mentioned subspaces and it can be divided into two parts

$$\mathcal{DE}^{\prec}_{\mathbf{u}} := \left\{\mathbf{v} \middle| \exists \mathbf{i} \subset \mathcal{M} : v_{\mathbf{i}} = u_{\mathbf{i}} \wedge \forall j \in \mathcal{M}\backslash\mathbf{i} : v_j \le u_j\right\} \tag{6}$$

$$\mathcal{DE}^{\succ}_{\mathbf{u}} := \left\{\mathbf{v} \middle| \exists \mathbf{i} \subset \mathcal{M} : v_{\mathbf{i}} = u_{\mathbf{i}} \wedge \forall j \in \mathcal{M}\backslash\mathbf{i} : v_j \ge u_j\right\} \tag{7}$$

herein, $\mathcal{DE}^{\prec}_{\mathbf{u}}$ is responsible for the subspace $\mathbf{\Lambda}^{\prec}_{\mathbf{u}}$ while $\mathcal{DE}^{\succ}_{\mathbf{u}}$ is responsible for the subspace $\mathbf{\Lambda}^{\succ}_{\mathbf{u}}$. It is worth noting that although the above definition is derived from CPO, it can be easily adapted to fit other Pareto-compatible optimality criteria.

Normally, $\mathbf{\Lambda}^{\prec}$ and $\mathcal{DE}^{\prec}$ are of most interest to users since they are closely related to the exploration capability of MOEAs. In Fig. 1(b), an expansion of the DE, $\mathcal{DE}^{\prec}$ (e.g., for solution B, $\mathcal{DE}^{\succ}_{\mathbf{B}}$ has been expanded to $B_1'BB_2'$ from B_1BB_2), can be easily observed. Another interesting observation in Fig. 1(b) is that, for both CPO and CDAS, the shapes of the DEs pertaining to different solutions are the same. Unfortunately, this feature does not hold for CDAS when the dimensionality of MOPs is higher than two. As illustrated in Fig. 2(b), the dominating space of each solution does get expanded with CDAS, but at the cost of changing their DEs differently. This implies that the optimality criterion provided by CDAS changes with solutions, which makes these solutions comparable only in a geometric sense. Therefore, a different generalization of CPO—one can not only control the dominating space as needed, but also ensure the identity of DEs for all solutions—is highly desired. Fig. 2(c) and (d) gives a symmetric and an asymmetric prototype of this desired generalization of CPO, respectively.

IV. Generalization of Pareto-Optimality

This section is devoted to presenting the generalization process of the proposed optimality criterion—i.e., GPO. Following the specific-to-general principle, a transformation equation similar to (2) is first constructed for the symmetric generalization, then it is further generalized for the asymmetric case. Finally, the differences between GPO and its predecessors (i.e., CPO and CDAS) are briefly discussed.

A. Symmetric Generalization of CPO

For optimality criteria without any preference, the importance of all dimensions should be equivalent. Thus, for the intended generalization, a specific solution with identical objective values (i.e., 1) in each dimension could be employed to represent the general case. In addition, only one arbitrary dimension needs to be taken into consideration when dealing with the symmetric case.

Analogous to CDAS, an objective value transformation equation is also required in GPO to allow an appropriate expansion to the dominating space of a solution. A rough description of the corresponding transformation equation is given by

$$f_i'(\mathbf{x}) = f_i(\mathbf{x}) + \Delta_i \quad i \in \mathcal{M} \tag{8}$$

where Δ_i is the objective increment in the ith dimension after the transformation. Obviously, Δ_i is closely linked to the expansion degree of the dominating space; and this parameter in CDAS is replaced by another one termed expanding degree $\boldsymbol{\varphi} = [\varphi_1, \varphi_2, \ldots, \varphi_M]^T$. As illustrated in Fig. 3, φ is the angle between two corresponding partitions of DEs before and after the expansion. For symmetric generalization, we have $\forall i \in \{1, 2, \ldots, M\} : \varphi_i = \varphi$. Here, dominating ratio (DR) is introduced to represent the relative size of the dominating space

$$\mathrm{DR} := \mathbf{\Lambda}^{\prec}/\mathbf{\Lambda}. \tag{9}$$

Unlike DE, DR is identical for different solutions if they adopt the same optimality criterion. Under the circumstance of CPO, DR is a function of the dimensionality of the MOP

$$\mathrm{DR}(M) = {}^{1}\!/_{2^M}. \tag{10}$$

It is easy to see that the DR of CPO decreases drastically as the number of objectives increases, which inexorably translates into a lack of selection pressure. Hence, a relatively constant DR, despite the change of problem dimensionality, is desired for GPO.

Two pictorial examples of symmetric dominating space expansions in spaces with different dimensionalities are presented in Fig. 3. Considering the mutual orthogonality of all dimensions and by resorting to the dimensional analogy method [63], we can calculate the unknown increment Δ_i in (8) as

$$\Delta_i = 1 \cdot \sqrt{M-1} \cdot \tan\varphi_i. \tag{11}$$

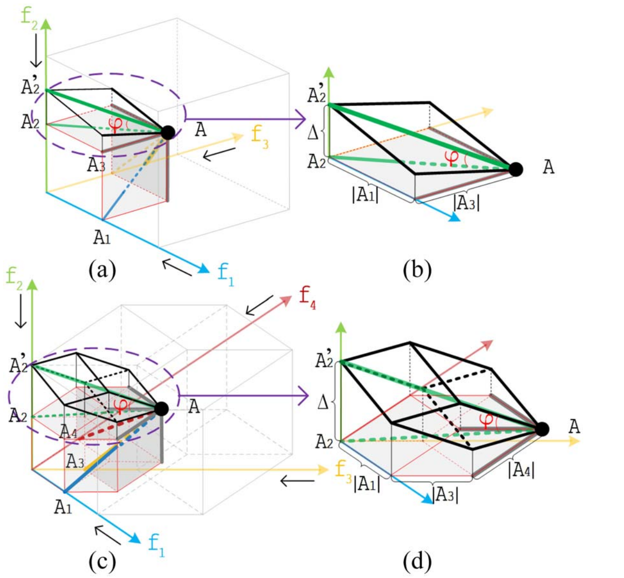

Fig. 3. Demonstrations of the dominating space expansion and the corresponding DE for solution A in the second dimension. (a) Partial dominating space expansion for A<1, 1, 1>. (b) Partially enlarged view on DE partitions of A<1, 1, 1>. (c). Partial dominating space expansion for A<1, 1, 1, 1>. (d) Partially enlarged view on DE partitions of A<1, 1, 1, 1>.

Therefore, for all solutions having arbitrary but identical objective values in each dimension, (8) can be rewritten as

$$f_i^{'}(\mathbf{x}) = f_i(\mathbf{x}) + f_i(\mathbf{x}) \cdot \sqrt{M-1} \cdot \tan\varphi_i \quad i \in \boldsymbol{\mathcal{M}}. \tag{12}$$

With the view of further extending the applicability of (12) to all solutions, the expanded view of the dominating space expansion with respect to dimension k in an M-dimensional space, as depicted in Fig. 4, is investigated. Fig. 4 reveals that the increment in dimension k consists of $(M-1)$ parts, and each of them stands for the response of every other dimension to the dominating space expansion. Still, for solutions with identical objective values in each dimension

$$f_i^{'}(\mathbf{x}) = f_i(\mathbf{x}) + \sum_{j=1}^{M-1} \left(f_i(\mathbf{x}) \cdot \sqrt{M-1} \cdot \tan\varphi_i \right) \Big/ (M-1) \quad i \in \boldsymbol{\mathcal{M}}. \tag{13}$$

Since all dimensions are uncorrelated due to their mutual orthogonality, each of them can be isolated from the others and regarded as a dimension of another solution which has the same objective values as the current one in every dimension. Thus, the final version of (8) can be inferred as

$$f_i^{'}(\mathbf{x}) = f_i(\mathbf{x}) + \sum_j \left(\delta_i \cdot f_j(\mathbf{x}) \right) \quad i \in \boldsymbol{\mathcal{M}}, j \in \boldsymbol{\mathcal{M}} \backslash \{i\} \tag{14}$$

$$\delta_i = \sqrt{M-1} \cdot \tan\varphi_i \big/ (M-1) \tag{15}$$

where δ_i is the expanding coefficient for the ith dimension, and this coefficient stands for the amount of gain in the ith objective for a loss of one unit in any other dimension.

Based on (14), we can redefine the concept of Pareto dominance in (2) as follows.

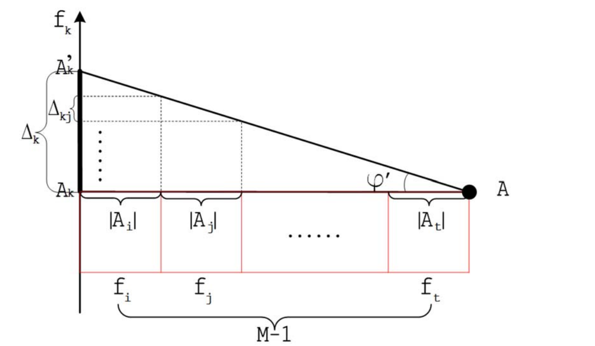

Fig. 4. Expanded view of the dominating space expansion with respect to dimension k in an M-dimensional space (generalized from Fig. 3).

Definition (Generalized Pareto Dominance): A solution $\mathbf{u} = [u_1, u_2, \ldots, u_M]^T$ is said to generally dominate another solution $\mathbf{v} = [v_1, v_2, \ldots, v_M]^T$ with respect to $\boldsymbol{\varphi} = [\varphi_1, \varphi_2, \ldots, \varphi_M]^T$ (denoted by $\mathbf{u} \preceq^{\boldsymbol{\varphi}} \mathbf{v}$) if and only if $\mathbf{u}^{\boldsymbol{\varphi}}$ is partially less than $\mathbf{v}^{\boldsymbol{\varphi}}$, that is

$$\mathbf{u} \preceq^{\boldsymbol{\varphi}} \mathbf{v} \Leftrightarrow \begin{cases} \forall i \in \boldsymbol{\mathcal{M}}, \forall k \in \boldsymbol{\mathcal{M}} \backslash \{i\} : u_i \\ \qquad \le v_i + \sum_k \delta_i \cdot (v_k - u_k) \\ \wedge\ \exists j \in \boldsymbol{\mathcal{M}}, \forall k \in \boldsymbol{\mathcal{M}} \backslash \{j\} : u_j \\ \qquad < v_j + \sum_k \delta_j \cdot (v_k - u_k) \end{cases} \tag{16}$$

where $\boldsymbol{\varphi} = [\varphi_1, \varphi_2, \ldots, \varphi_M]^T$ and $\delta_i = \sqrt{M-1} \cdot \tan\varphi_i/(M-1)$.

Similarly, the DE in (5) can be redefined as follows.

Definition (Generalized Dominance Envelope): For a given solution $\mathbf{u} = [u_1, u_2, \ldots, u_M]^T$ within $\boldsymbol{\Lambda} \subset \mathbb{R}^M$, the generalized dominance envelope (GDE) pertaining to $\mathbf{u}$ with respect to $\boldsymbol{\varphi} = [\varphi_1, \varphi_2, \ldots, \varphi_M]^T$ (denoted by $\boldsymbol{\mathcal{DE}}_{\mathbf{u}}^{\boldsymbol{\varphi}}$) is the set of all solutions that are equal to $\mathbf{u}^{\boldsymbol{\varphi}}$ in terms of at least 1-D, that is

$$\boldsymbol{\mathcal{DE}}_{\mathbf{u}}^{\boldsymbol{\varphi}} := \left\{ v \,\middle|\, \exists i \in \boldsymbol{\mathcal{M}}, \forall j \in \boldsymbol{\mathcal{M}} \backslash \{i\} : \frac{u_i - v_i}{\sum_j (v_j - u_j)} = \delta_i \right\} \tag{17}$$

where $\mathbf{v} = [v_1, v_2, \ldots, v_M]^T$ is an arbitrary solution within $\boldsymbol{\Lambda}$, $\boldsymbol{\varphi} = [\varphi_1, \varphi_2, \ldots, \varphi_M]^T$, and $\delta_i = \sqrt{M-1} \cdot \tan\varphi_i/(M-1)$.

The generalized versions of other Pareto-based concepts are not provided here; but they may be analogically rendered as needed.

Although GPO seems to be very close to α-dominance and guided-dominance considering their similar weighted-sum technique for CPO relaxation, it has a lower difficulty in parameter setting. By taking advantage of the DE expansion, GPO has successfully reduced the unknown parameters from $M(M-1)$ weight coefficients representing pairwise tradeoffs among objectives to M expanding angles $\boldsymbol{\varphi}$ controlling the dimension-wise dominance area expansions. Clearly, $\mathbf{0}$ is the lower bound of $\boldsymbol{\varphi}$, and GPO is exactly the same as CPO when $\boldsymbol{\varphi} = \mathbf{0}$. However, the upper bound of $\boldsymbol{\varphi}$ for a given problem dimensionality is still unknown.

Claim 1: Given an M-dimensional space and the symmetric generalization of Pareto-optimality, the maximum possible value for every component in $\boldsymbol{\varphi}$ is $\arctan(\sqrt{M-1})$ with DR = 0.5.

Proof: By definition, DR is directly proportional to the size of the dominating space $\boldsymbol{\Lambda}^{\prec}$, and the latter is a monotonically

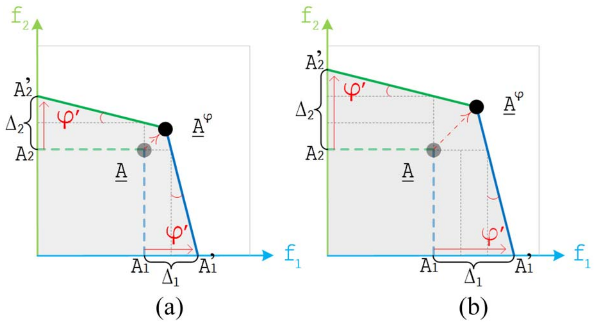

Fig. 5. Symmetric generalization process (in Fig. 3) projected onto a 2-D main plane $[f_1–f_2]$, $\underline{A}$ and $\underline{A}^{\boldsymbol{\varphi}}$ are projections of the solution A before and after the generalization. (a) 3-D case. (b) 4-D case.

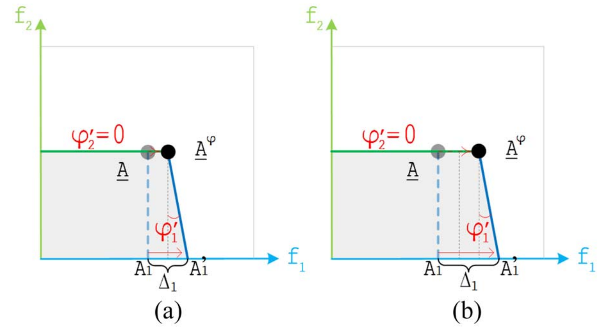

Fig. 6. Asymmetric generalization process (no expansion in second dimension) projected onto a 2-D main plane $[f_1 - f_2]$, $\underline{A}$ and $\underline{A}^{\boldsymbol{\varphi}}$ are projections of the solution A before and after the generalization. (a) 3-D case. (b) 4-D case.

increasing function of $\boldsymbol{\varphi}$. This suggests that the upper bound of $\boldsymbol{\varphi}$ with respect to a specific dimensionality is the vector that can maximize DR. Moreover, the sizes of $\boldsymbol{\Lambda}^{\prec}$ and $\boldsymbol{\Lambda}^{\succ}$ are equal due to their duality, and a non-null intersection of these two subspaces is contradictory—i.e., a solution in the intersection would both dominate and be dominated by another solution at the same time. Therefore, DR reaches its maximum (0.5) when the GDE $\mathcal{DE}^{\boldsymbol{\varphi}\prec}$ is a hyper-plane. Projecting the dominating space onto an arbitrary 2-D main plane, as in Fig. 5, which represents a 3-D and a 4-D case in (a) and (b), respectively, it can be seen that when $\mathcal{DE}^{\boldsymbol{\varphi}\prec}$ is expanded to a hyper-plane, the corresponding expanding coefficient reaches 1, which is also its maximum. This result simply gives the allowed maximum value for every component in $\boldsymbol{\varphi}$, that is

$$\varphi_M^{\max} = \arctan\left(\sqrt{M-1}\cdot\delta_{\max}\right) = \arctan\left(\sqrt{M-1}\right). \quad (18)$$

Claim 2: Given an M-dimensional space $\boldsymbol{\Lambda}$ and the symmetric generalization of Pareto-optimality, if $\boldsymbol{\varphi}_1$ and $\boldsymbol{\varphi}_2$ are two expanding vectors which satisfy $\{\boldsymbol{\varphi}_1, \boldsymbol{\varphi}_2\} \in [0, \varphi_M^{\max})$ and $\boldsymbol{\varphi}_1 < \boldsymbol{\varphi}_2$, and $\mathbf{u} = [u_1, u_2, \ldots, u_M]^T$ and $\mathbf{v} = [v_1, v_2, \ldots, v_M]^T$ are two arbitrary solutions in $\boldsymbol{\Lambda}$, then

$$\mathbf{u} \preceq^{\boldsymbol{\varphi}_1} \mathbf{v} \underset{\times}{\rightleftharpoons} \mathbf{u} \preceq^{\boldsymbol{\varphi}_2} \mathbf{v} \quad (19)$$

$$\mathbf{u} \sim^{\boldsymbol{\varphi}_1} \mathbf{v} \overset{\times}{\rightleftharpoons} \mathbf{u} \sim^{\boldsymbol{\varphi}_2} \mathbf{v} \quad (20)$$

where $\sim^{\boldsymbol{\varphi}}$ is the generalized nondominated relation. Based on the definition in (16) of generalized Pareto dominance, (19) and (20) can be easily proved.

B. Asymmetric Generalization of CPO

AGPO is just a further generalized form of CPO based on symmetric generalization of CPO (SGPO). Fig. 6(a) and (b) gives two instances of asymmetric generalization in a 3-D and a 4-D space, respectively. To transfer from SGPO, one need only relax the requirement for identical expanding in every dimension. As a consequence, the upper bounds for different components of $\boldsymbol{\varphi}$ are no longer necessarily the same.

C. Differences Between GPO and CPO

Since GPO is Pareto-compatible, it follows the same qualitative pattern with CPO—i.e., a solution cannot achieve a "better" value for one of the objectives without "worsening" at least one other. But when it comes to the quantitative description, they are not quite the same. There exists a kind of inherent internal compromise among different dimensions in GPO—it allows a solution to dominate another while its objective value in a certain dimension is comparatively disadvantageous. This just corresponds to the standpoint in economics that Pareto-optimal is only a minimal notion of optimality [42]. In other words, CPO is not a sufficient but a necessary condition for being optimal in some sense.

As mentioned, DR is much related to the selection pressure of an optimality criterion. For CPO, the DR is constant when the problem dimensionality is specified. However, under the circumstance of GPO, DR changes with not only the problem dimensionality but also the expanding degree. This leads to the much more flexible and higher selection pressure of GPO. Furthermore, the discriminability pertaining to different dimensions can be altered individually by assigning different expanding degrees.

For GPO, it holds that the selection pressure gets boosted, but, in turn, problems may arise concerning diversity preservation. Given a nondominated solution set, some of them may become dominators of the others by taking advantage of the internal compromise among different dimensions in GPO, resulting in a search bias toward a certain region of the true Pareto front in the selection process that ensues. A graphical explanation could be the indirect contraction of the objective space. As shown in Fig. 7, a marked difference—i.e., the coverage rate of the true Pareto front—between the conventional Pareto front (shown by a bold curve) and the generalized Pareto front (shown by arc PQ) can be clearly observed. In fact, the larger the expanding degree is, the lower the coverage rate of the true Pareto front might be. When the expanding degree reaches its maximum, the objective space will be transformed into a hyper-line, and there is only one solution left in the generalized Pareto front in this extreme case.

D. Differences Between GPO and CDAS

GPO can be regarded as an amendment to CDAS since both of them transform the objective values of solutions to control their dominance areas. To put them in a unified analysis

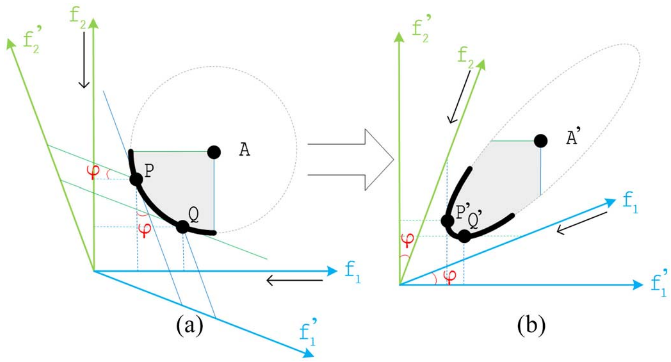

Fig. 7. Pictorial demonstration of the contraction of a 2-D objective space and the shrink of the generalized Pareto front after generalizing the Pareto-optimality. (a) Original objective space. (b) Contracted objective space after generalization.

framework, (4) can be rewritten as

$$f_i^{'}(\mathbf{x}) = f_i(\mathbf{x}) + \sqrt{\sum_j f_j^2} \cdot \tan\varphi_i \quad i \in \boldsymbol{\mathcal{M}},\ j \in \boldsymbol{\mathcal{M}} \backslash \{i\}. \quad (21)$$

For the purpose of comparing GPO and CDAS in a numerical sense, one need only compare the second items of (14) and (21), and it is not difficult to prove that

$$\sqrt{\sum_k f_k^2} - \sum_k f_k \bigg/ \sqrt{M-1} \geq 0 \quad k \in \{1, 2, \ldots, M-1\}. \quad (22)$$

Clearly, (22) only equals zero in the following situations: 1) the dimensionality of the problem is two and 2) the objective values of a solution are identical with respect to all dimensions. In other cases, for an arbitrary solution, the transformed objective values of CDAS are always higher than those of GPO, provided the expanding degrees are the same.

In addition, the expanding coefficient of CDAS can be extracted from (21)

$$\delta_i^{'} = \left(\sqrt{\sum_j f_j^2} \cdot \tan\varphi_i\right) \bigg/ \sum_j f_j \quad i \in \boldsymbol{\mathcal{M}}, j \in \boldsymbol{\mathcal{M}} \backslash \{i\}. \quad (23)$$

Compared with (15), (23) has no correlations with the problem dimensionality, but rather with the objective values of solutions. Namely, it varies solution by solution, this explains why the $\boldsymbol{\mathcal{DE}}^{\prec}$ of different solutions in Fig. 2(b) are quite disparate.

V. STATIC ANALYSES OF GPO

In this section, we use some isolated artificial datasets to statically analyze GPO. The DR surface of GPO is first delineated to assist the selection of appropriate expanding angle. Then, with the help of the nondominated sorting technique [3], the rank distribution and the ranking landscape of GPO over some benchmark problems are investigated.

A. Benchmark Problems

Three well-known test problems (i.e., DTLZ1, DTLZ2, and DTLZ7) with different geometrical characteristics of the Pareto-optimal fronts are chosen to make comparisons between different optimality criteria. They are selected for this paper because they all share the following important features: 1) generic enough to be scaled to any number of objectives and decision variables; 2) convergence and diversity difficulties can be easily controlled by the so-called multimodal function; 3) the global Pareto front is known analytically; and 4) they are unconstrained, since constraint handling lies beyond the scope of this investigation. More specifically, DTLZ1-2 both challenge the convergence ability of MOEAs to approach the true Pareto front by introducing a huge but controlled number of local optima. The optimal Pareto front of DTLZ1 is a linear hyper-plane while that of DTLZ2 is a concave surface of a hyper-sphere. To provide more complete and reliable comparison results, DTLZ2 is modified for a convex optimal Pareto front (details are given in [64]), and this modified test problem is referred to as DTLZ2.5 hereinafter. As for DTLZ7, it has multiple disconnected Pareto-optimal regions to test the ability of maintaining subpopulations in disconnected portions of the objective space. Please refer to [65] for more detailed information about these benchmarks.

B. DR Surface

By generalizing CPO, GPO is capable of providing nondiscriminatory expansion of the DE for any solution. This furnishes us with the flexibility of regulating the selection pressure, embodied in the size of the dominating space, of optimizers within a certain range, thereby making it possible to improve the scalability of MOEAs via maintaining the evolutionary pressure as the number of objectives increases.

However, without the knowledge of how DR varies with different problem dimensionalities and expanding angles, only subjective regulations of the selection pressure could be expected. To the best of our knowledge, there exists only one related work [37] which attempts to analytically describe the DR of CDAS in

$$\mathrm{DR} = \left\{\frac{1}{2} - \left(\frac{1}{2}\right)^M\right\} \cdot \left(\varphi \middle/ \frac{\pi}{4}\right)^{M-1} + \left(\frac{1}{2}\right)^M \quad (24)$$

where M is the problem dimensionality, and φ is the expanding angle. Unfortunately, the applicability of (24) is limited to only 2-D problems, even for CDAS, due to its assumption concerning the proportional relationship between DR and φ.

In this section, the correlations among DR, problem dimensionality, and expanding angles are experimentally investigated for both SGPO and CDAS. To ensure the homogeneity of all directions for simulating a borderless space, a hypersphere space, rather than a hyper-cube one, is employed. Estimating the DR value essentially involves the calculation of a cone-based hypervolume [66], and for efficiency, it is here conducted by the Monte Carlo method. The following steps,

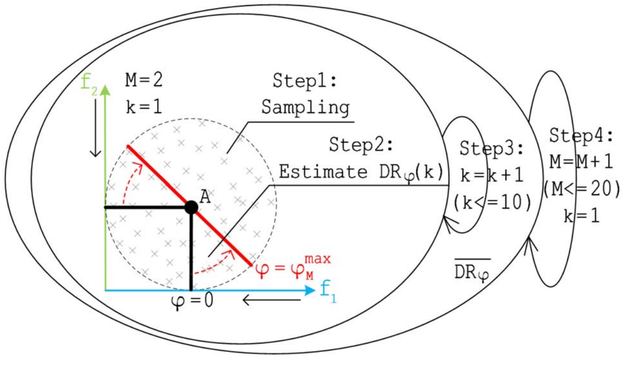

Fig. 8. Illustration of the steps for DR estimation.

as illustrated in Fig. 8, were performed to obtain the DRs of the hyper-sphere center A.

Step 1: For a specific dimensionality m, uniformly sample the corresponding hyper-sphere space for a cloud dataset of size 100 000.

Step 2: Calculate the DRs of the hyper-sphere center with respect to all the expanding degrees which are linearly sampled from the interval [0, $\varphi_m^{\max}$] for both SGPO and CDAS.

Step 3: Repeat steps 1 and 2 ten times, and for each expanding degree considered, average the DRs resulting from different cloud datasets and record the averaged value.

Step 4: Iterate the previous steps until all the dimensionalities ranging from 2 to 20 have been examined.

The DR surfaces of SGPO and CDAS are, respectively, shown in Fig. 9(a) and (b), from which at least the following points can be summed up: 1) given the same expanding degree, the DR decreases with increasing dimensionalities, and the higher the dimension, the smaller the decreasing gradient; 2) when the dimensionality increases above two, the linear relationship between the DR and the expanding degree cannot be maintained; 3) for problems with a dimensionality higher than two, the DR of CDAS is always lower than that of SGPO, and so is the growth of DR for increasing expanding degrees; 4) unlike that of SGPO, the DR of CDAS is not a monotonically increasing function of the expanding degree if the dimensionality is higher than two, and its maximum decreases with increasing dimensionality.

With the DR surface of SGPO, one need only single out an appropriate expanding angle and use it to generalize CPO when a certain level of selection pressure is desired for a given problem dimensionality. Fig. 10 extracts the expanding angles corresponding to some special values (i.e., 0.125, 0.25, and 0.5) from Fig. 9(a). Since the main focus of the scalability extension is to inherit the excellent performance of CPO from low-dimensional spaces to high-dimensional ones, we suggest a pseudo-2-D principle to guide the parameter selection. Specifically, the DR value of CPO for 2-D problems (i.e., 0.25) is taken as a benchmark for the expansion control with respect to any problem dimensionality. For example, by referring to the red square marks in Fig. 10, the expected expanding angle for 3-D problems is 19.5 if the aforementioned principle is to be followed.

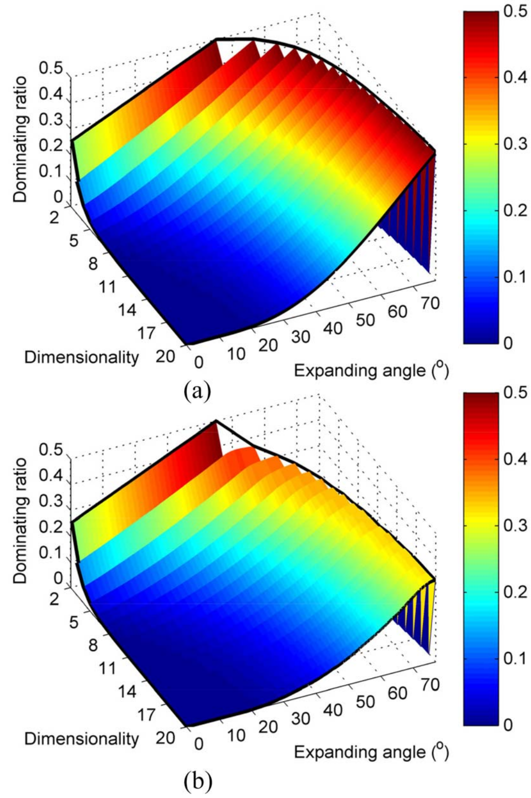

Fig. 9. Variations in DR with the problem dimensionality and the expanding angle of the dominating space. DR surface of (a) SGPO and (b) CDAS.

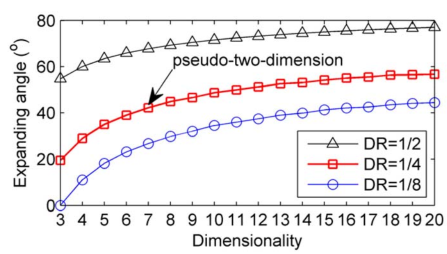

Fig. 10. Expanding angles settings for different combinations of problem dimensionality and the desired DR.

C. Rank Distribution

One criterion to estimate the quality of a ranking method is to analyze the distribution of the ranks assigned to a set of solutions. In general, a ranking method will have a positive impact on the selection process if it is able to subdivide the population more finely to generate a richer range of ranks. Without a variety of ranks, an optimizer will lose its efficiency since it cannot maintain the search pressure.

Only when provided with a tangible population of a specific problem, can we investigate the distribution of ranks for different ranking schemes. Here, rather than random or earlier populations, later populations of the evolutionary process are focused for analysis. The reason lies in the fact that most ranking schemes are incomparable in terms of rank variety in the early stage of evolution, but when the population marches toward the Pareto optima, some of them, e.g., CPO, will become inefficient due to their progressive loss of rank diversity.

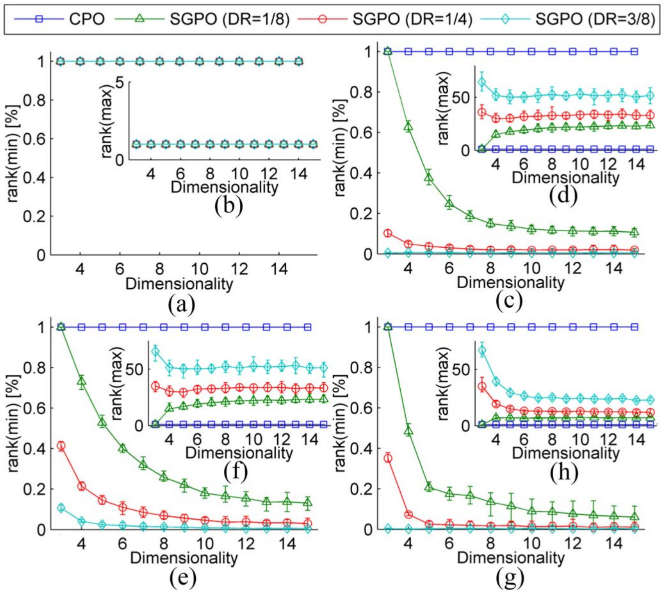

Fig. 11. Distribution of ranks of near-optimal populations for DTLZ problems in spaces with different dimensionalities and DRs. (a) Proportion of solutions with minimum rank for DTLZ1. (b) Maximum rank for DTLZ1. (c) Proportion of solutions with minimum rank for DTLZ2. (d) Maximum rank for DTLZ2. (e) Proportion of solutions with minimum rank for DTLZ2.5. (f) Maximum rank for DTLZ2.5. (g) Proportion of solutions with minimum rank for DTLZ7. (h) Maximum rank for DTLZ7.

The rank distribution presented in this section belongs to the nondominance ranking of some near-optimal populations of the four benchmark problems. These experiments were performed in spaces with dimensionalities ranging from 3 to 15 and a moderate population size (i.e., 500) was selected. The DR of SGPO was set as 0.125, 0.25, and 0.375 to check its influence on the rank variety which is measured by the proportion of solutions with the minimum rank and the maximum nondominance rank. To get an averaged result, each experiment was independently performed 30 times.

As given in Fig. 11, CPO becomes powerless as the proportion of solutions with the minimum rank reaches 100% and the selection procedure under this circumstance relies merely on the diversity criterion. Concerning this issue, SGPO has indeed shown better dimensional scalability. Except for DTLZ1, the results of SGPO over other test problems indicate that: 1) given a certain problem dimensionality, the greater the DR, the better the rank variety (i.e., fewer solutions with the minimum rank and higher the maximum nondominance rank) and 2) given a certain DR, the higher the problem dimensionality, the lower the ratio of solutions with the minimum rank. Fig. 11 also shows an obvious result difference between DTLZ1 and other problems, this difference implies that SGPO does provide the flexibility of regulating the solution discriminability by fixing different DRs, but it may come at the cost of leaving out some Pareto-optimal solutions. However, any algorithm using a diversity criterion runs this risk to some extent.

D. Ranking Landscape

Similar to the fitness landscape used in single-objective optimization, it is possible to visualize the behavior of a ranking method by introducing another form of rank distribution—the ranking landscape. A ranking landscape is created by plotting decision variables against the ranks assigned to each point of the decision space. Since solutions with lower ranks gain better chances to reproduce, the population will be guided toward the valley of the ranking landscape.

One of the issues with the method of creating the ranking landscape is that the number of decision variables should be limited to two for making visualization possible. For DTLZ problems, the number of decision variables (n) has the following relationship with the problem dimensionality (M) and a so-called difficulty factor (k) : $n = M + k - 1$. Therefore, the ranking landscapes of these problems can be visually examined, but only by limiting the evolutionary difficulty. Namely, we can examine the ranking landscape of Pareto-optimal fronts of 3-D DTLZ problems. Under this circumstance, the ranking landscape is a plateau with the "height" of one for CPO, but for GPO, there may also exist peaks and valleys. This should be attributed to their ranking bias corresponding to different shapes of the Pareto front. Thus, the ranking landscapes allow us to see what kind of solutions a ranking method prefers and to which subset of the Pareto-optimal front it might converge.

In this section, the ranking biases of SGPO and AGPO are investigated. Since they are related to the shape of the Pareto-optimal front, 3-D DTLZ1, DTLZ2, DTLZ2.5, and DTLZ7 are all employed to represent problems with plane, concave, convex, and disconnected Pareto fronts. The expansion degree, if any, is set to 19.5 for these problems.

Fig. 12 shows the meshed plots of ranking landscapes based on SGPO accompanied by the corresponding objective spaces of these benchmark problems. In landscape plots, the dark blue areas stands for the optimal set that SGPO will converge to, and their counterparts are marked with red squares in the objective space. As CPO is only a special case of SGPO, we can assert that these areas will shrink as DR increases. Clearly, SGPO has different ranking biases when dealing with different Pareto fronts. For DTLZ1, SGPO has the same result as CPO. As for DTLZ2.5, it only favors the most balanced solutions; however, when it comes to DTLZ2, it also rewards the solutions at the edges of the Pareto front. Although having a disconnected Pareto front, the ranking result for DTLZ7 can still be regarded as similar to that of DTLZ2.

The ranking landscape of AGPO is also explored, as shown in Fig. 13. Compared with Fig. 12(b), while the partial expansion of the dominating space impairs the rank variety, it enlarges the dark blue areas in landscape plots. And extra peaks are generated as the number of expanding dimensions increases. In the objective space, it is clear that the survivability of solutions with respect to a dimension decreases as the expanding angle corresponding to this dimension increases.

VI. Evolutionary Analyses of GPO

The static analyses reveal that GPO has the potential of promoting convergence with increased solution discriminability, but it may also impair the diversity of the final solution set at the same time. To further investigate its convergence

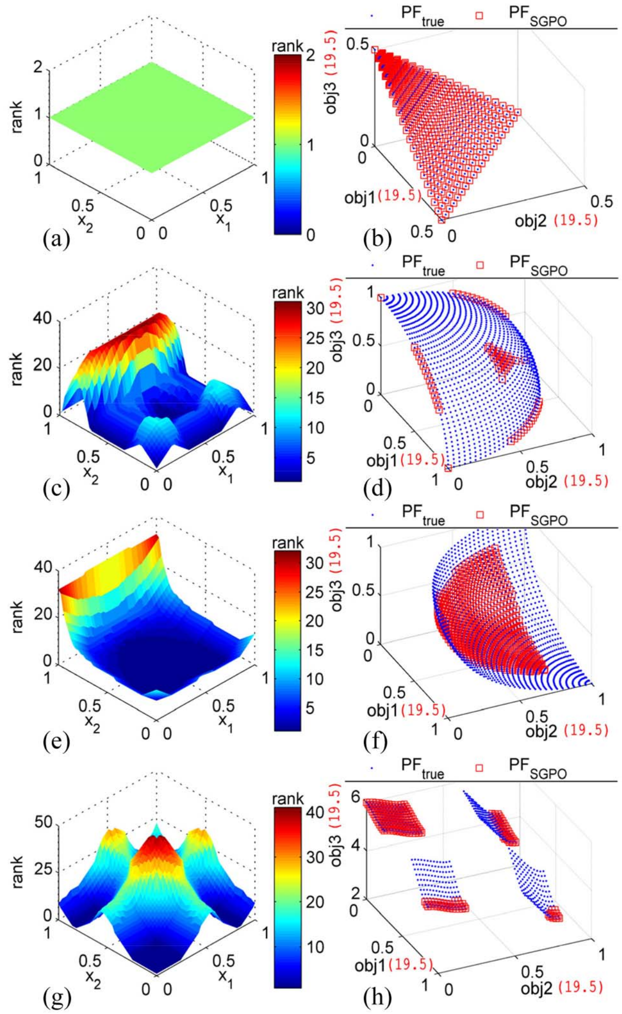

Fig. 12. SGPO-based ranking landscapes and the corresponding objective spaces of problems with different shapes of the Pareto fronts (expanding angles are provided within brackets). (a) Landscape plot of DTLZ1. (b) Objective space of DTLZ1. (c) Landscape plot of DTLZ2. (d) Objective space of DTLZ2. (e) Landscape plot of DTLZ2.5 (derived from DTLZ2). (f) Objective space of DTLZ2.5. (g) Landscape plot of DTLZ7. (h) Objective space of DTLZ7.

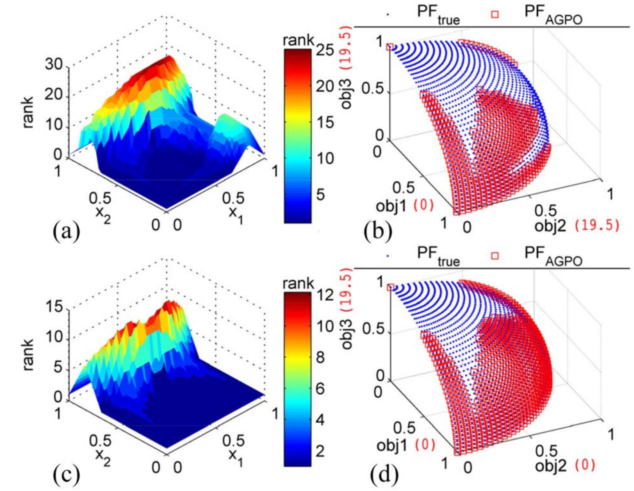

Fig. 13. AGPO-based ranking landscapes and the corresponding objective spaces of problem DTLZ2 with different expanding angles (provided within brackets). (a) Landscape plot of DTLZ2 (without expansion in the first dimension). (b) Objective space of DTLZ2 with two expanded dimensions. (c) Landscape plot of DTLZ2 (with expansion in the third dimension). (d) Objective space of DTLZ2 with only one expanded dimension.

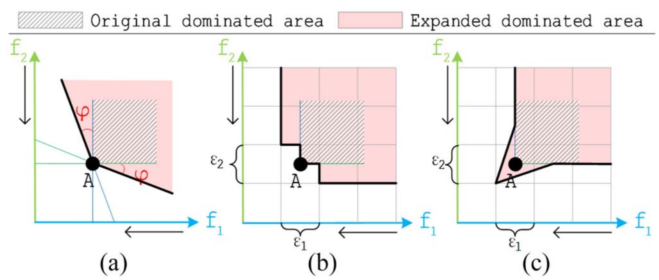

Fig. 14. Dominance area modification techniques of different optimality criteria. (a) SGPO. (b) ε-dominance. (c) Cone ε-dominance.

contribution and possible diversity shortage, GPO is incorporated into MOEAs and comparatively studied with some other optimality criteria in this section.

A. Algorithms in Comparison

As the most popular MOEA in the literature, NSGA-II is employed as an algorithm shell to comparatively assess the performances of both CPO and GPO through its ranking procedure. The choice of NSGA-II is mainly motivated by two reasons: 1) its widespread use in different areas and 2) its poor scalability performance with respect to number of objectives, as compared with some other MOEAs [67].

For comparison purpose, two other state-of-the-art MOEAs, i.e., ε-MOEA [59] and cone ε-MOEA [60], are also considered. As depicted in Fig. 14, the optimality criteria—i.e., ε-dominance and cone ε-dominance—adopted in these two algorithms are quite close to GPO since they all modify the dominance area of solutions. However, their underlying mechanisms are not the same, as they require a gridding process [see Fig. 14(b) and (c)].

To provide a comparison baseline, all algorithms are implemented within the MATLAB platform and some common parameter settings are adopted: the operators for crossover and mutation are simulated binary crossover and polynomial mutation with both distribution indices set to 20 (i.e., $\eta_c = 20$ and $\eta_m = 20$); their probabilities are set to 1.0 and 1/N (i.e., $p_c = 0.1$ and $p_m = 1/N$, where N is the number of decision variables), respectively [1]. Moreover, each algorithm is independently run 30 times on every test problem in all the following experiments.

B. Performance Metrics

Almost all MOEAs are devoted to converging to the Pareto-optimal front and maintaining as much solution diversity as possible at the same time. Considering this multicriterion nature in the evaluation of multiobjective algorithms, we have introduced three different metrics in our analysis.

The convergence metric Υ [3] is employed to measure the distance between the obtained nondominated front $P(t)$ at each

TABLE I
ESTIMATED PARAMETER ε TO ROUGHLY GET AN ARCHIVE SIZE OF 500 FOR 5-D DTLZ PROBLEMS

	DTLZ1	DTLZ2	DTLZ2.5	DTLZ7
ε-MOEA	0.0405	0.1225	0.1225	0.1169
Cone ε-MOEA	0.1150	0.2495	0.3000	0.4550

generation t and a detailed sampling of the true Pareto-optimal front P^*

$$\Upsilon(P(t)) = \sum_{i=1}^{|P(t)|} d_i \Big/ |P(t)| \tag{25}$$

where d_i is the smallest normalized Euclidean distance, in the objective space, between each solution i in $P(t)$ and P^*. So, the lower the Υ value, the better the convergence of the solutions in $P(t)$.

The diversity metric Δ [3] is adopted to measure the extent of spread achieved among the obtained nondominated solutions in $P(t)$

$$\Delta(P(t)) = \left(\sum_{m=1}^{M} d_m^e + \sum_{i=1}^{|P(t)|} \left|d_i - \bar{d}\right|\right) \Big/ \left(\sum_{m=1}^{M} d_m^e + |P(t)|\bar{d}\right) \tag{26}$$

where d_m^e denotes the Euclidean distance between the extreme solutions of P^* and $P(t)$ corresponding to the mth objective function, d_i is the averaged distance of each solution in $P(t)$ to its Mth nearest neighboring solutions, and $\bar{d}$ is the mean value of d_i. So the lower the Δ value, the better the distribution of solutions.

As a metric estimating both convergence and diversity of the obtained solutions, hypervolume H [68] is also used in this paper. It calculates the hypervolume enclosed by the achieved front P and a reference point dominated by all solutions in this front. So the larger the dominated hypervolume, the better the front is. For all test problems, the reference point is set as 10% greater than the upper boundaries of the Pareto-optimal front. Since the exact calculation of the hypervolume metric is computationally expensive, we approximate the hypervolume result of a solution set by the Monte Carlo sampling method [69] with a sampling size of 1 000 000.

C. Convergence Validation

To understand how the optimality criteria affect the convergence ability of MOEAs, we need to investigate how different ranking schemes and corresponding populations behave by observing evolution in action.

In this experiment, 5-D DTLZ problems with a population size of 500 are employed, and the termination criterion is a maximum generation of 500. Aiming at an archive size of 500 solutions in 5-D objective spaces, the estimated ε values listed in Table I are used for ε-MOEA and cone ε-MOEA.

Fig. 15 shows the evolving dynamics of the convergence metric on problem DTLZ1. Clearly, the SGPO-based NSGA-II has both fastest convergence speed and best approximation of the Pareto-optimal front. Although the dominance area of solutions does get expanded in cone ε-dominance, there is not much advantage of cone ε-MOEA over the CPO-based NSGA-II on this test problem; on the contrary, the latter sometimes outperforms the former. According to the result on DTLZ2 in Fig. 16, the ε-MOEA and the cone ε-MOEA have the similar convergence dynamics and both of them outperform the CPO-based NSGA-II. However, the SGPO-based NSGA-II is still the algorithm with the best convergence behavior on this test problem. In the case of DTLZ2.5, the convergence dynamics of all algorithms, even the CPO-based NSGA-II, are alike with only minor differences, as shown in Fig. 17. When it comes to the result on DTLZ7 in Fig. 18, the SGPO-based NSGA-II still possesses an apparent advantage over both CPO-based NSGA-II and cone ε-MOEA, while CPO-based NSGA-II remains the algorithm with the worst convergence performance.

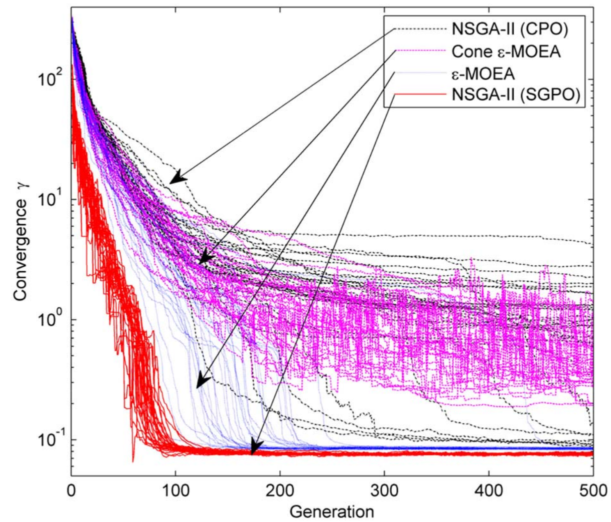

Fig. 15. Evolutionary dynamics of the convergence metric for different algorithms on problem DTLZ1.

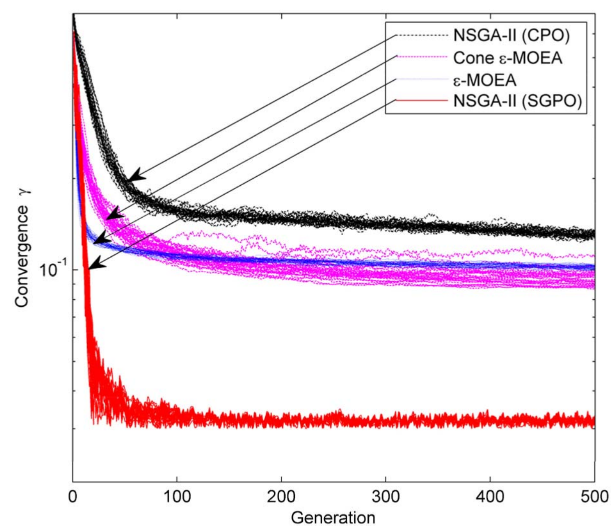

Fig. 16. Evolutionary dynamics of the convergence metric for different algorithms on problem DTLZ2.

Table II tabulates the values of the diversity metric for the final solution set of every algorithm on each test problem. Except for DTLZ1, the SGPO-based NSGA-II has the worst solution diversity on every other test problem. Similar results

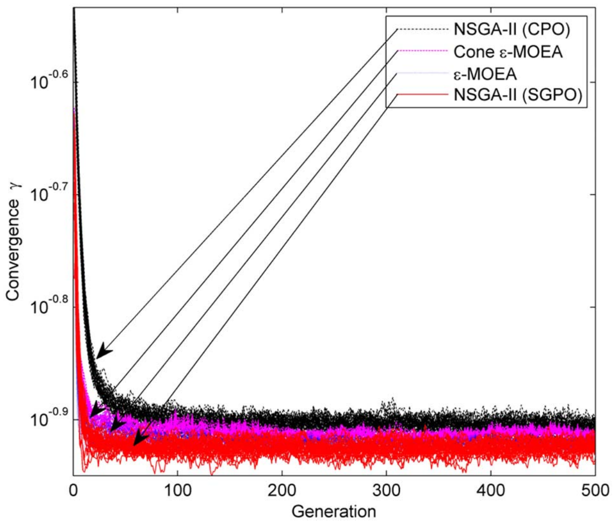

Fig. 17. Evolutionary dynamics of the convergence metric for different algorithms on problem DTLZ2.5 (derived from DTLZ2).

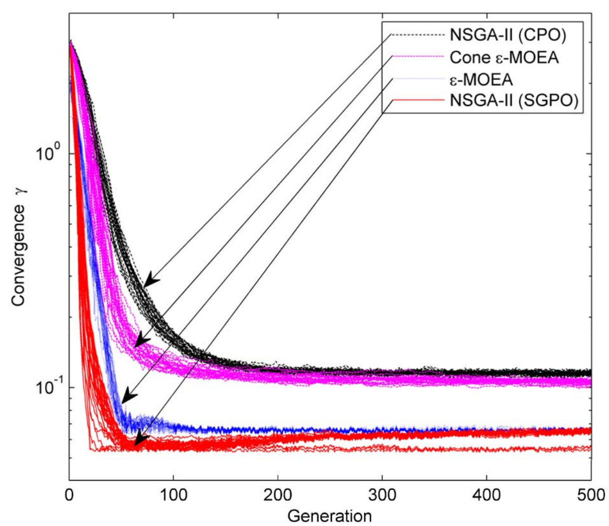

Fig. 18. Evolutionary dynamics of the convergence metric for different algorithms on problem DTLZ7.

can be found in Table III, which lists the hypervolume metrics for all the final solution sets. Although the SGPO-based NSGA-II has the best convergence on all the test problems considered, the aggregative quality of its final solutions still gets compromised due to its diversity shortage.

D. Diversity Compensation

For those who expect MOEAs to converge to the complete Pareto front, GPO is an "aggressive" optimality criterion. It furnishes MOEAs with a much faster convergence rate and better scalability, but mostly at the cost of introducing to MOEAs some difficulty in diversity maintenance by converging to subsets of the Pareto-optimal front. Regular diversity preservation strategies (e.g., niche, crowding, and clustering [1]) are powerless to address this inherent search bias since they affect only those attainable solutions.

In light of the results presented in Fig. 13, we suggest an evolutionary framework called distributed evolution as a

TABLE II

AVERAGED DIVERSITY METRICS AND THEIR STANDARD DEVIATIONS (WITHIN BRACKETS) OF THE FINAL POPULATIONS GENERATED BY DIFFERENT ALGORITHMS ON 5-D DTLZ PROBLEMS

	DTLZ1	DTLZ2	DTLZ2.5	DTLZ7
NSGA-II (CPO)	4.8293E-1 (5.0475E-2)	2.7519E-1 (3.5059E-2)	2.6195E-1 (1.8828E-2)	4.6657E-1 (4.0441E-2)
NSGA-II (SGPO)	4.6062E-1 (4.6061E-2)	7.4216E-1 (2.3122E-2)	3.0340E-1 (6.9915E-2)	5.8061E-1 (5.7678E-2)
ε-MOEA	9.5530E-2 (7.7903E-3)	1.1346E-1 (4.0085E-3)	1.3608E-1 (7.3975E-3)	3.5509E-1 (2.3654E-2)
Cone ε-MOEA	6.2625E-1 (4.3532E-1)	7.8301E-2 (5.6889E-3)	1.3175E-1 (5.8241E-3)	3.1304E-1 (1.3263E-2)

TABLE III

AVERAGED HYPERVOLUME METRICS AND THEIR STANDARD DEVIATIONS (WITHIN BRACKETS) OF THE FINAL POPULATIONS GENERATED BY DIFFERENT ALGORITHMS ON 5-D DTLZ PROBLEMS

	DTLZ1	DTLZ2	DTLZ2.5	DTLZ7
NSGA-II (CPO)	4.5940E-1 (3.8606E-1)	8.7891E-1 (7.5261E-3)	8.0008-1 (1.0481E-2)	8.1194E-1 (6.4320E-3)
NSGA-II (SGPO)	9.9419E-1 (6.9417E-4)	8.7217E-1 (3.2400E-2)	8.2259-1 (5.4055E-3)	2.6744E-1 (7.7010E-2)
ε-MOEA	9.5967E-1 (6.1608E-3)	9.8181E-1 (1.6653E-3)	8.8310-1 (5.7310E-3)	7.7293E-1 (3.2504E-2)
Cone ε-MOEA	9.7317E-1 (4.3692E-2)	9.9764E-1 (1.3594E-3)	8.7455-1 (5.8831E-3)	9.0559E-1 (3.4907E-3)

compensating effort for acquiring the entire Pareto front. The basic idea of this distributed evolution technique is to evolve the Pareto front in parallel with multiple processors. Since the evolutionary search can be biased toward particular regions of the Pareto front by resorting to AGPO with appropriate parameter settings, it is possible to distribute the task of finding the entire Pareto front to multiple subtasks, and allocate each of them to different processors.

Regarding the task distribution, two conditions must be satisfied: 1) the entire Pareto front should be covered and 2) the overlap of regions allocated to any two processors should be minimized. The first issue can be easily ensured either by reducing the "aggressiveness" of AGPO or increasing the quantity of processors. However, the second issue is much tougher as it is affected not only by the aforementioned two factors but also by the shape of the Pareto front.

For problems with convex Pareto-optimal fronts, a chopping principle [64], which requires an aggregated dominating hyper-plane to "chop-off" the bottom-left corner of the objective space, can be followed to make sure of the strict satisfaction of the above two conditions. To this end, the problem dimensionality is set as the quantity of processors for distributed evolution, and the dominance area expansion in each processor is restricted to only 1-D, but with the maximum expanding angle given in (18). This complementary parameter choice is graphically explained and instantiated in Figs. 19 and 20, respectively. Clearly, with customized expansion in different processors, this chopping technique can exactly divide the task of approximating the Pareto-optimal front AC into the subtasks of finding BC and AB separately. Unfortunately, however, this technique only works perfectly for convex fronts; when it comes to concave or

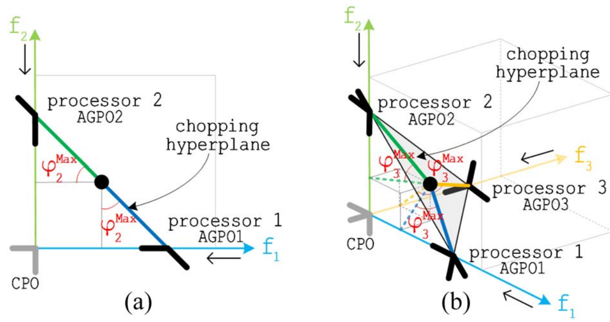

Fig. 19. Illustration of the chopping technique for distributed evolution and its AGPO-based construction examples. (a) Chopping hyperplane aggregation in a 2-D space. (b) Chopping hyperplane aggregation in a 3-D space.

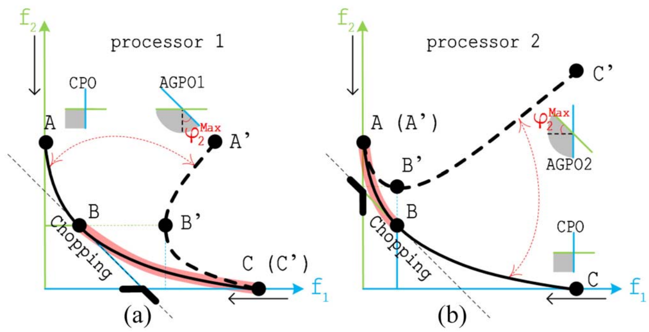

Fig. 20. Illustration of the distributed evolution on different processors in a 2-D space. (a) Processor 1 evolves with only maximum expansion in the first dimension. (b) Processor 2 evolves with only maximum expansion in the second dimension.

disconnected situations, it often fails miserably as neither of the aforementioned conditions can be guaranteed.

To extend the versatility of the chopping technique, an adaptive parameter setting strategy is further introduced, as described in Table IV. Based on the gridding of the objective space [61] with a spatial resolution of 50 in every dimension, this strategy employs an extra master processor to estimate the diversity of the aggregated solution set by tallying the grids occupied and overlapped. The expanding angle is first initialized according to the chopping principle to generate a relatively high selection pressure at the early stage of evolution, then, for a maximized occupancy with a minimum overlap, it is correspondingly adjusted to adapt to the changes of the gridding metrics until the evolution is terminated.

For ease of visualization, 3-D DTLZ problems with a population size of 300 are additionally adopted for this experiment. The ε values for ε-MOEA and cone ε-MOEA in this case are listed in Table V. The maximum generations for both 3-D and 5-D problems are set to 1000 to ensure the convergence of the population.

Fig. 21 presents the result of a typical run of the proposed distributed evolution strategy on the 3-D DTLZ1 problem. As expected, the Pareto fronts of all the three processors are mutually overlapped in Fig. 21(b), which explains why the diversity metrics and the expanding angle all remain relatively stable after the subpopulations become mutually nondominated in Fig. 21(a). However, the diversity behavior of the 3-D DTLZ2, as depicted in Fig. 22, is quite different. For concave

TABLE IV
PSEUDO CODE OF GRID-BASED PARAMETER ADAPTATION ALGORITHM FOR DISTRIBUTED EVOLUTION

Input: nondominated subpopulations, expanding angle φ
Output: expanding angle φ'

```
Aggregate subpopulations and update grid parameters if needed;
Rasterize the objective space;
Tally grids occupied N_occupy and overlapped N_overlap ;
Check convergence by examining recent fluctuations σ of N_occupy ;
if (nominally converged)
  if (first nominal convergence)
    φ' = φ − 1, k = 1;
    Save reference occupancy R_occupy and overlap R_overlap ;
    Randomly migrate solutions among subpopulations;
  else
    if ( N̄_occupy − (2 − k)·σ > R_occupy ) {occupancy improvement}
      φ' = φ − 1, k = 1;
      Update reference occupancy R_occupy and overlap R_overlap ;
      Randomly migrate solutions among subpopulations;
    else
      if ( k < 2 ) {first occupancy-improvement detection}
        k = k + 1; {give it another try with looser restrictions}
      else {occupancy saturation confirmed}
        if ( N_overlap > R_overlap ) {overlap increment detected}
          φ' = φ + 0.5 , k = 1;
          Randomly migrate solutions among subpopulations;
        else {no occupancy improvement or overlap increment}
          φ' = φ − 0.5 ;
        end if
      end if
    end if
  end if
end if
```

TABLE V
ESTIMATED PARAMETER ε TO ROUGHLY GET ARCHIVE SIZE OF 300 FOR 3-D DTLZ PROBLEMS

	DTLZ1	DTLZ2	DTLZ2.5	DTLZ7
ε-MOEA	0.0200	0.0340	0.0340	0.0275
Cone ε-MOEA	0.0360	0.0890	0.0910	0.0990

Pareto fronts, the spread of solutions is very limited at the start of the evolution, then it grows as the expanding angle decreases. After the occupancy reaches its maximum, the expanding angle starts to fluctuate within a small range to balance the occupancy and the overlap. The compound population plotted in Fig. 22(b) reveals that the distributed evolution strategy perfectly satisfies the above-mentioned two task-distribution conditions. For the case of the 3-D DTLZ2.5 in Fig. 23, although there is no need to modify the expanding angle, it still slightly fluctuates for higher occupancy or lower overlap. Fig. 24 is the result corresponding to the 3-D DTLZ7. In this case of a disconnected Pareto front, the master processor has to continuously lower the expanding angle to 0 for maximum occupancy without taking the overlap into consideration.

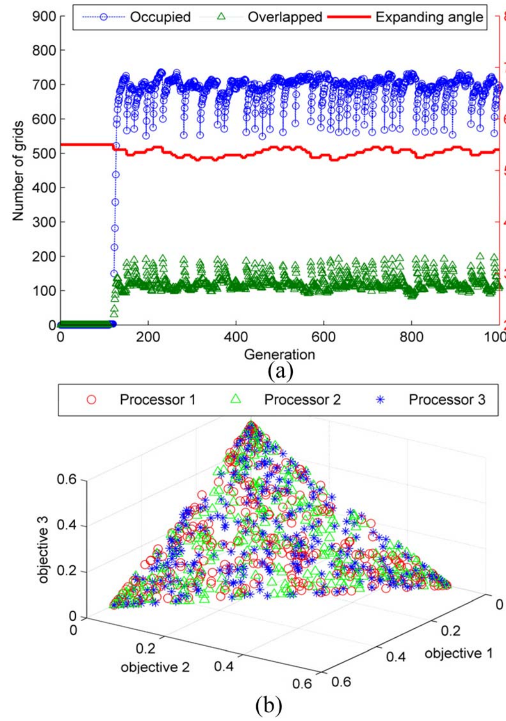

Fig. 21. Result of a typical evolutionary run of the distributed evolution on the 3-D problem DTLZ1. (a) Evolutionary dynamics of the occupancy, the overlap, and the expanding angle. (b) Objective space plot of the final compound population aggregated from all processors.

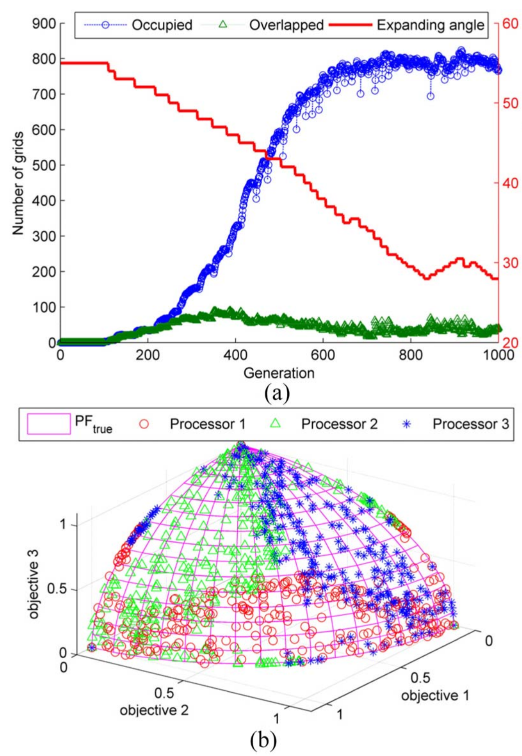

Fig. 22. Result of a typical evolutionary run of the distributed evolution on the 3-D problem DTLZ2. (a) Evolutionary dynamics of the occupancy, the overlap, and the expanding angle. (b) Objective space plot of the final compound population aggregated from all processors.

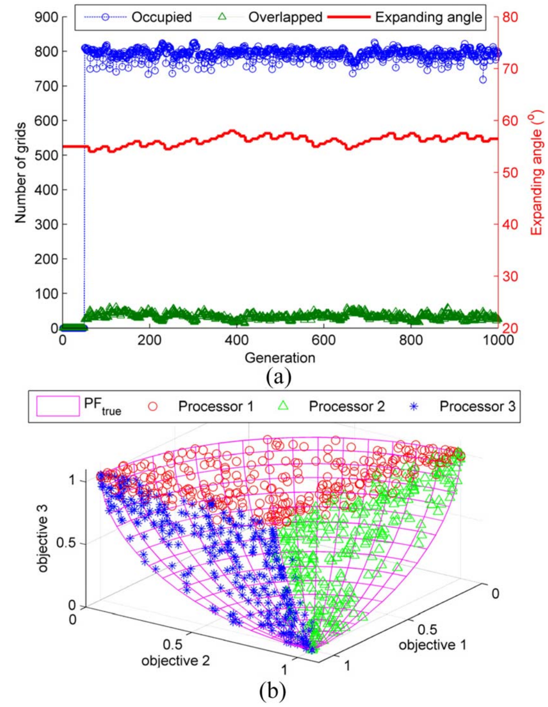

Fig. 23. Result of a typical evolutionary run of the distributed evolution on the 3-D problem DTLZ2.5 (derived form DTLZ2). (a) Evolutionary dynamics of the occupancy, the overlap, and the expanding angle. (b) Objective space plot of the final compound population aggregated from all processors.

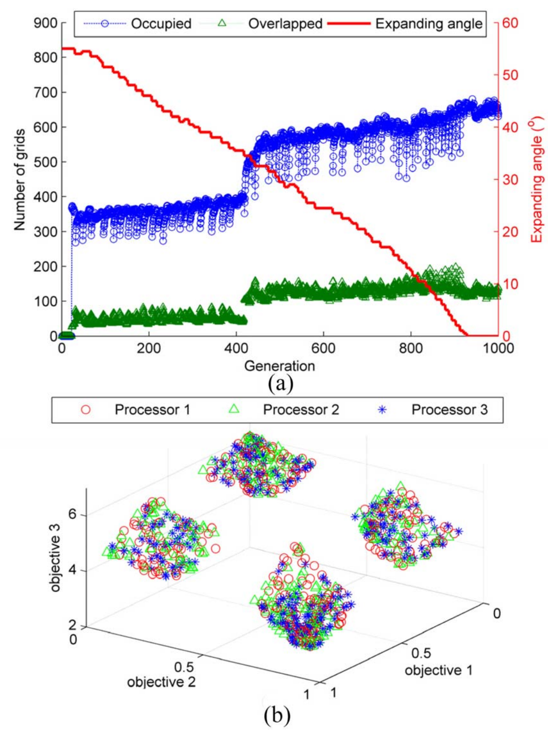

Fig. 24. Result of a typical evolutionary run of the distributed evolution on the 3-D problem DTLZ7. (a) Evolutionary dynamics of the occupancy, the overlap, and the expanding angle. (b) Objective space plot of the final compound population aggregated from all processors.

Besides the intuitive analyses of the diversity improvement for 3-D DTLZ problems in the above figures, the convergence, diversity, and the hypervolume of the final compound populations are also statistically studied in Tables VI–VIII, respectively. Although the AGPO-based distributed NSGA-II is not as good as the SGPO-based NSGA-II in terms of

TABLE VI
AVERAGED CONVERGENCE METRICS AND THEIR STANDARD DEVIATIONS (WITHIN BRACKETS) OF THE FINAL POPULATIONS GENERATED BY DIFFERENT ALGORITHMS ON 3-D DTLZ PROBLEMS

	DTLZ1	DTLZ2	DTLZ2.5	DTLZ7
NSGA-II (CPO)	1.8148E-2 (7.6237E-3)	2.0390E-2 (4.1665E-4)	1.8592E-2 (4.3053E-4)	1.4307E-2 (7.0920E-4)
NSGA-II (SGPO)	1.4300E-2 (1.6142E-3)	1.3376E-2 (2.1887E-4)	1.7778E-2 (3.5323E-4)	8.1120E-3 (1.6427E-4)
ε-MOEA	1.6042E-2 (2.8224E-3)	1.8598E-2 (3.1836E-4)	1.8889E-2 (3.0481E-4)	9.9748E-3 (1.8864E-4)
Cone ε-MOEA	7.4858E-2 (2.8614E-2)	1.7169E-2 (5.8165E-4)	1.8598E-2 (2.6783E-4)	1.5110E-2 (4.5633E-4)
NSGA-II (AGPO)	1.4973E-2 (1.0751E-4)	1.7734E-2 (1.9861E-4)	1.7501E-2 (1.5437E-4)	1.3555E-2 (3.2076E-4)

TABLE VII
AVERAGED DIVERSITY METRICS AND THEIR STANDARD DEVIATIONS (WITHIN BRACKETS) OF THE FINAL POPULATIONS GENERATED BY DIFFERENT ALGORITHMS ON 3-D DTLZ PROBLEMS

	DTLZ1	DTLZ2	DTLZ2.5	DTLZ7
NSGA-II (CPO)	5.0449E-1 (3.5848E-2)	3.3984E-1 (7.7441E-2)	3.5231E-1 (4.4505E-2)	6.4856E-1 (5.2800E-2)
NSGA-II (SGPO)	5.0148E-1 (5.7639E-2)	6.5015E-1 (1.0150E-1)	4.3684E-1 (6.8176E-2)	7.0344E-1 (5.8472E-2)
ε-MOEA	1.2074E-1 (1.6669E-2)	2.4535E-1 (7.2253E-3)	2.7191E-1 (2.1573E-2)	3.1064E-1 (3.3466E-2)
Cone ε-MOEA	2.4019E-1 (3.1375E-1)	1.1565E-1 (7.1504E-3)	2.0858E-1 (1.5923E-2)	2.7670E-1 (2.2821E-2)
NSGA-II (AGPO)	2.4936E-1 (7.9697E-3)	2.6857E-1 (1.5645E-2)	3.0644E-1 (3.7706E-2)	3.2055E-1 (1.2198E-2)

TABLE VIII
AVERAGED HYPERVOLUME METRICS AND THEIR STANDARD DEVIATIONS (WITHIN BRACKETS) OF THE FINAL POPULATIONS GENERATED BY DIFFERENT ALGORITHMS ON 3-D DTLZ PROBLEMS

	DTLZ1	DTLZ2	DTLZ2.5	DTLZ7
NSGA-II (CPO)	9.7300E-1 (9.1134E-3)	9.4823E-1 (3.7420E-3)	9.5843E-1 (3.7586E-3)	9.6642E-1 (4.2088E-3)
NSGA-II (SGPO)	9.7816E-1 (3.2624E-3)	9.0714E-1 (2.4648E-3)	9.4650E-1 (1.8943E-3)	8.9347E-1 (3.2885E-3)
ε-MOEA	9.7161E-1 (6.0058E-3)	9.7997E-1 (2.5985E-3)	9.7523E-1 (2.6048E-3)	9.7202E-1 (4.2566E-3)
Cone ε-MOEA	9.8773E-1 (2.1543E-3)	9.8395E-1 (2.9020E-3)	9.8395E-1 (2.9020E-3)	9.7967E-1 (3.2292E-3)
NSGA-II (AGPO)	9.9734E-1 (1.6962E-3)	9.8654E-1 (2.6661E-3)	9.8946E-1 (4.4017E-3)	9.9013E-1 (3.2831E-3)

TABLE IX
AVERAGED DIVERSITY AND HYPERVOLUME METRICS WITH THEIR STANDARD DEVIATIONS (WITHIN BRACKETS) OF THE FINAL POPULATIONS GENERATED BY THE DISTRIBUTED EVOLUTION ON 5-D DTLZ PROBLEMS

	DTLZ1	DTLZ2	DTLZ2.5	DTLZ7
Δ	2.7430E-1 (1.0247E-2)	1.1229E-1 (3.5140E-3)	1.6247-1 (5.2574E-3)	1.9447E-1 (6.1541E-3)
H	9.9832E-1 (4.3754E-4)	9.8787E-1 (2.2090E-3)	9.8630E-1 (6.8022E-3)	9.0521E-1 (4.2546E-3)

convergence ability, it still can generate competitive approximations of the Pareto optima with similar diversity and better hypervolume compared with the other algorithms. The diversity and hypervolume metrics of the final compound populations on 5-D DTLZ problems are also provided in Table IX. By referring to Tables II and III, it is easy to see that the solution diversity does improve greatly using the proposed distributed evolution.

VII. CONCLUSION

Aiming at improving the scalability of Pareto-based MOEAs, this paper generalized the Pareto-optimality both symmetrically and asymmetrically by providing nondiscriminatory expansions of the dominance area of solutions. With the aid of these generalizations, MOEAs could acquire the flexibility of changing their selection pressures within certain ranges, which would allow them to maintain their evolvability when dealing with problems with many objectives. The GPO was compared with its original version in terms of the distribution of ranks, the ranking landscape and the rate of convergence to the Pareto optima on several DTLZ problems. According to the experimental results, the algorithm equipped with the proposed optimality criterion could not only achieve a richer variety of ranks but also attain faster and better convergence to the true Pareto front.

However, the experiments also showed that the possible ranking bias induced by the generalization might cause a diversity maintenance difficulty. Although it might not be necessarily considered to be a drawback under some circumstances, a scheme to mitigate it was still proposed: a distributed evolution framework with adaptive parameter settings. This strategy distributed the diversity maintenance task to multiple coevolved populations by resorting to the search bias of the asymmetrically GPO, and its parameter adaptively changed when dealing with problems with different shapes of Pareto-optimal fronts. This distributed evolution technique was empirically proved to be promising in improving diversity preservation related to MOEAs associated with GPO.

Note that no attempt has been made to enumerate and compare more parameter specification strategies for GPO in this paper. For those who only value the convergence performance of MOEAs, a dictionary-like "pseudo-2-D" principle is provided to keep the DR value constant across a range of problem dimensionalities, and for those who are concerned about the possible diversity loss induced by the generalization, an adaptive chopping principle is available to compensate the diversity performance of MOEAs within a distributed evolution framework. However, there still exist some restrictions (e.g., selection of the expected DR level and quantity of the processors for distributed evolution) that affect the applicability of these strategies. Therefore, as part of future work, some more generalized cases need to be further investigated to fully exploit the potential of GPO.

REFERENCES

[1] K. Deb, *Multi-Objective Optimization Using Evolutionary Algorithms*. Chichester, U.K.: Wiley, 2001.

[2] C. A. C. Coello, G. B. Lamont, and D. A. Van Veldhuizen, *Evolutionary Algorithms for Solving Multi-Objective Problems*, 2nd ed. New York, NY, USA: Springer, Sep. 2007.

[3] K. Deb, A. Pratap, S. Agarwal, and T. Meyarivan, "A fast and elitist multiobjective genetic algorithm: NSGA-II," *IEEE Trans. Evol. Comput.*, vol. 6, no. 2, pp. 182–197, Apr. 2002.

[4] E. Zitzler, M. Laumanns, and L. Thiele, "SPEA2: Improving the strength Pareto evolutionary algorithm," in *Proc. EUROGEN Evol. Methods Design Optim. Control Appl. Ind. Probl.*, Athens, Greece, 2001, pp. 1–21.

[5] C. Fonseca and P. Fleming, "Genetic algorithms for multiobjective optimization: Formulation, discussion and generalization," in *Proc. 5th Int. Conf. Genet. Algorithms*, vol. 1. San Francisco, CA, USA, 1993, pp. 416–423.

[6] J. Horn, N. Nafpliotis, and D. Goldberg, "A niched Pareto genetic algorithm for multiobjective optimization," in *Proc. IEEE CEC*, Orlando, FL, USA, 1994, pp. 82–87.

[7] E. Zitzler and L. Thiele, "Multiobjective evolutionary algorithms: A comparative case study and the strength Pareto approach," *IEEE Trans. Evol. Comput.*, vol. 3, no. 4, pp. 257–271, Nov. 1999.

[8] N. Srinivas and K. Deb, "Multiobjective optimization using nondominated sorting in genetic algorithms," *Evol. Comput.*, vol. 2, no. 3, pp. 221–248, 1994.

[9] J. Knowles and D. Corne, "The Pareto archived evolution strategy: A new baseline algorithm for Pareto multiobjective optimization," in *Proc. IEEE CEC*, vol. 1. Washington, DC, USA, 1999, pp. 98–105.

[10] D. Corne, N. Jerram, J. Knowles, and M. Oates, "PESA-II: Region-based selection in evolutionary multiobjective optimization," in *Proc. GECCO*, San Francisco, CA, USA, 2001, pp. 283–290.

[11] C. A. C. Coello and M. Lechuga, "MOPSO: A proposal for multiple objective particle swarm optimization," in *Proc. IEEE CEC*, vol. 2. Honolulu, HI, USA, 2002, pp. 1051–1056.

[12] I. Karahan and M. Koksalan, "A territory defining multiobjective evolutionary algorithms and preference incorporation," *IEEE Trans. Evol. Comput.*, vol. 14, no. 4, pp. 636–664, Aug. 2010.

[13] D. Corne and J. Knowles, "Techniques for highly multiobjective optimization: Some non-dominated points are better than others," in *Proc. GECCO*, London, U.K., 2007, pp. 773–780.

[14] J. Knowles and D. Corne, "Quantifying the effects of objective space dimension in evolutionary multiobjective optimization," in *Evolutionary Multi-Criterion Optimization* (LNCS 4403). Berlin, Germany: Springer, 2007, pp. 757–771.

[15] O. Teytaud, "How entropy-theorems can show that approximating high-dim Pareto-fronts is too hard," in *Proc. Bridg. Gap Between Theory Pract.—Workshop PPSN-BTP*, Reykjavik, Iceland, 2006, pp. 1–14.

[16] E. J. Hughes, "Evolutionary many-objective optimization: Many once or one many?" in *Proc. CEC*, vol. 1. Edinburgh, U.K., 2005, pp. 222–227.

[17] V. Khare, X. Yao, and K. Deb, "Performance scaling of multi-objective evolutionary algorithms," in *Evolutionary Multi-Criterion Optimization* (LNCS 2632). Berlin, Germany: Springer, 2003, pp. 376–390.

[18] K. Praditwong and X. Yao, "How well do multi-objective evolutionary algorithms scale to large problems," in *Proc. IEEE CEC*, Singapore, 2007, pp. 3959–3966.

[19] T. Wagner, N. Beume, and B. Naujoks, "Pareto-, aggregation-, and indicator-based methods in many-objective optimization," in *Evolutionary Multi-Criterion Optimization* (LNCS 4403). Berlin, Germany: Springer, 2007, pp. 742–756.

[20] W. Mkaouer, M. Kessentini, S. Bechikh, K. Deb, and M. Ó Cinnéide, "High dimensional search-based software engineering: Finding tradeoffs among 15 objectives for automating software refactoring using NSGA-III," COIN, Dept. Mech. Eng., Indian Inst. Technol., Kanpur, India, Tech. Rep. 2013002, 2013. [Online]. Available: http://www.egr.msu.edu/~kdeb/papers/c2013002.pdf

[21] M. Farina and P. Amato, "A Fuzzy definition of optimality for many-criteria optimization problems," *IEEE Trans. Syst., Man, Cybern. A, Syst., Humans*, vol. 34, no. 3, pp. 315–326, May 2004.

[22] S. Bandyopadhyay and A. Mukherjee, "An algorithm for many-objective optimization with reduced objective computations: A study in differential evolution," *IEEE Trans. Evol. Comput.*, vol. 19, no. 3, pp. 400–413, Jun. 2015.

[23] H. K. Singh, A. Isaacs, and T. Ray, "A Pareto corner search evolutionary algorithm and dimensionality reduction in many-objective optimization problems," *IEEE Trans. Evol. Comput.*, vol. 15, no. 4, pp. 539–556, Aug. 2011.

[24] Q. Zhang and H. Li, "MOEA/D: A multiobjective evolutionary algorithm based on decomposition," *IEEE Trans. Evol. Comput.*, vol. 11, no. 6, pp. 712–731, Dec. 2007.

[25] H. Liu, F. Gu, and Q. Zhang, "Decomposition of a multiobjective optimization problem into a number of simple multiobjective subproblems," *IEEE Trans. Evol. Comput.*, vol. 18, no. 3, pp. 450–455, Jun. 2014.

[26] M. Asafuddoula, T. Ray, and R. Sarker, "A decomposition-based evolutionary algorithm for many objective optimization," *IEEE Trans. Evol. Comput.*, vol. 19, no. 3, pp. 445–460, Jun. 2015.

[27] L. B. Said, S. Bechikh, and K. Ghedira, "The r-dominance: A new dominance relation for interactive evolutionary multi-criteria decision making," *IEEE Trans. Evol. Comput.*, vol. 14, no. 5, pp. 801–818, Oct. 2010.

[28] L. Thiele, K. Miettinen, P. J. Korhonen, and J. M. Luque, "A preference-based evolutionary algorithm for multi-objective optimization," *Evol. Comput.*, vol. 17, no. 3, pp. 411–436, 2009.

[29] K. Deb, J. Sundar, N. Uday, and S. Chaudhuri, "Reference point based multi-objective optimization using evolutionary algorithms," *Int. J. Comput. Intell. Res.*, vol. 2, no. 6, pp. 273–286, 2006.

[30] R. Wang, R. C. Purshouse, and P. J. Fleming, "Preference-inspired coevolutionary algorithms for many-objective optimization," *IEEE Trans. Evol. Comput.*, vol. 17, no. 4, pp. 474–494, Aug. 2013.

[31] K. Deb and H. Jain, "An evolutionary many-objective optimization algorithm using reference-point based non-dominated sorting approach, part I: Solving problem with box constraints," *IEEE Trans. Evol. Comput.*, vol. 18, no. 4, pp. 577–601, Aug. 2014.

[32] H. Jain and K. Deb, "An evolutionary many-objective optimization algorithm using reference-point-based nondominated sorting approach, part II: Handling constraints and extending to an adaptive approach," *IEEE Trans. Evol. Comput.*, vol. 18, no. 4, pp. 602–622, Aug. 2014.

[33] K. Ikeda, H. Kita, and S. Kobayashi, "Failure of Pareto-based MOEAs: Does non-dominated really mean near to optimal?" in *Proc. IEEE CEC*, Seoul, Korea, 2001, pp. 957–962.

[34] H. Sato, H. E. Aguirre, and K. Tanaka, "Controlling dominance area of solutions and its impact on the performance of MOEAs," in *Evolutionary Multi-Criterion Optimization* (LNCS 4403). Berlin, Germany: Springer, 2007, pp. 5–20.

[35] H. Sato, H. E. Aguirre, and K. Tanaka, "Self-controlling dominance area of solutions in evolutionary many-objective optimization," in *Simulated Evolution and Learning* (LNCS 6457). Berlin, Germany: Springer, 2010, pp. 455–465.

[36] H. Sato, H. Aguirre, and K. Tanaka, "Improved S-CDAs using crossover controlling the number of crossed genes for many-objective optimization," in *Proc. 13th Annu. Conf. Genet. Evol. Comput.*, Dublin, Ireland, 2011, pp. 753–760.

[37] K. Narukawa, "Effect of dominance balance in many-objective optimization," in *Evolutionary Multi-Criterion Optimization* (LNCS 7811). Berlin, Germany: Springer, 2013, pp. 276–290.

[38] J. Branke, T. Kaußler, and H. Schmeck, "Guidance in evolutionary multiobjective optimization," *Adv. Eng. Softw.*, vol. 32, no. 6, pp. 499–507, Jun. 2001.

[39] H. Aguirre and K. Tanaka, "Space partitioning with adaptive ε-ranking and substitute distance assignments: A comparative study on many-objective MNK-landscapes," in *Proc. 11th Annu. Conf. Genet. Evol. Comput.*, Montreal, QC, Canada, 2009, pp. 547–554.

[40] A. L. Jaimes, C. A. C. Coello, H. Aguirre, and K. Tanaka, "Adaptive objective space partitioning using conflicts information for many-objective optimization," in *Proc. Evol. Multi-Criter. Optim.*, Ouro Preto, Brazil, 2011, pp. 151–165.

[41] I. Das, "A preference ordering among various Pareto optimal alternatives," *Struct. Optim.*, vol. 18, no. 1, pp. 30–35, Aug. 1999.

[42] F. di Pierro, S. Khu, and D. A. Savic, "An investigation on preference order ranking scheme for multiobjective evolutionary optimization," *IEEE Trans. Evol. Comput.*, vol. 11, no. 1, pp. 17–45, Feb. 2007.

[43] V. D. Noghin, "Relative importance of criteria: A quantitative approach," *J. Multi-Criteria Decis. Anal.*, vol. 6, no. 6, pp. 355–363, Jan. 1997.

[44] Z. He, G. Yen, and J. Zhang, "Fuzzy-based Pareto optimality for many-objective evolutionary algorithms," *IEEE Trans. Evol. Comput.*, vol. 18, no. 2, pp. 269–285, Apr. 2014.

[45] M. Li, J. Zheng, K. Li, Q. Yuan, and R. Shen, "Enhancing diversity for average ranking method in evolutionary many-objective optimization," in *Proc. 11th Int. Conf. Parallel Probl. Solv. Nat.*, Kraków, Poland, 2010, pp. 647–656.

[46] P. J. Bentley and J. P. Wakefield, "Finding acceptable solutions in the Pareto-optimal range using multiobjective genetic algorithms," in *Soft Computing in Engineering Design and Manufacturing*. London, U.K.: Springer, 1998, pp. 231–240.

[47] S. Kukkonen and J. Lampinen, "Ranking-dominance and many-objective optimization," in *Proc. Congr. Evol. Comput.,* Singapore, 2007, pp. 3983–3990.

[48] N. Drechsler, R. Drechsler, and B. Becker, "Multi-objective optimization in evolutionary algorithms using satisfiability classes," in *Computational Intelligence* (LNCS 1625). Berlin, Germany: Springer, 1999, pp. 108–117.

[49] A. Sulflow, N. Drechsler, and R. Drechsler, "Robust multiobjective optimization in high dimensional spaces," in *Proc. Evol. Multi-Criter. Optim.*, Matsushima, Japan, 2007, pp. 715–726.

[50] K. Maneeratana, K. Boonlong, and N. Chaiyaratana, "Compressed-objective genetic algorithm," in *Proc. 9th Int. Conf. Parallel Probl. Solv. Nat.*, Reykjavik, Iceland, 2006, pp. 473–482.

[51] M. Garza-Fabre, G. Toscano-Pulido, and C. A. C. Coello, "Two novel approaches for many-objective optimization," in *Proc. Congr. Evol. Comput.*, Barcelona, Spain, 2010, pp. 1–8.

[52] E. Jara, "Multi-objective optimization by using evolutionary algorithms: The p-optimality criteria," *IEEE Trans. Evol. Comput.*, vol. 18, no. 2, pp. 167–179, Apr. 2014.

[53] X. Zou, Y. Chen, M. Liu, and L. Kang, "A new evolutionary algorithm for solving many-objective optimization problems," *IEEE Trans. Syst., Man, Cybern. B, Cybern.*, vol. 38, no. 5, pp. 1402–1412, Oct. 2008.

[54] E. J. Hughes, "Multiple single objective Pareto sampling," in *Proc. Congr. Evol. Comput.*, vol. 4. Canberra, ACT, Australia, 2003, pp. 2678–2684.

[55] E. J. Hughes, "Many-objective directed evolutionary line search," in *Proc. 13th Annu. Conf. Genet. Evol. Comput.*, Dublin, Ireland, 2011, pp. 761–768.

[56] J. Bader and E. Zitzler, "HypE: An algorithm for fast hypervolume based many-objective optimization," *Evol. Comput.*, vol. 19, no. 1, pp. 45–76, 2011.

[57] E. Zitzler and S. Kunzli, "Indicator-based selection in multiobjective search," in *Proc. Parallel Probl. Solv. Nat. (PPSN)*, Birmingham, U.K., 2004, pp. 831–842.

[58] N. Beume, B. Naujoks, and M. Emmerich, "SMS-EMOA: Multiobjective selection based on dominated hypervolume," *Eur. J. Oper. Res.*, vol. 181, no. 3, pp. 1653–1669, Sep. 2007.

[59] M. Laumanns, L. Thiele, K. Deb, and E. Zitzler, "Combining convergence and diversity in evolutionary multi-objective optimization," *Evol. Comput.*, vol. 10, no. 3, pp. 263–282, 2002.

[60] L. S. Batista, F. Campelo, F. G. Guimaraes, and J. A. Ramirez, "Pareto cone ε-dominance: Improving convergence and diversity in multiobjective evolutionary algorithms," in *Evolutionary Multi-Criterion Optimization* (LNCS 6576). Berlin, Germany: Springer, 2011, pp. 76–90.

[61] S. Yang, M. Li, and J. Zheng, "A grid-based evolutionary algorithm for many-objective optimization," *IEEE Trans. Evol. Comput.*, vol. 17, no. 5, pp. 721–736, Oct. 2013.

[62] A. L. Jaimes and C. A. C. Coello, "Study of preference relations in many-objective optimization," in *Proc. 11th Annu. Conf. Genet. Evol. Comput.*, Montreal, QC, Canada, 2009, pp. 611–618.

[63] M. Kaku, *Hyperspace: A Scientific Odyssey Through Parallel Universes, Time Warps, and the Tenth Dimension.* New York, NY, USA: Oxford Univ. Press, 1994.

[64] K. Deb, P. Zope, and A. Jain, "Distributed computing of Pareto-optimal solutions using multi-objective evolutionary algorithms," Kanpur Genet. Algorithms Lab., Indian Inst. Technol. Kanpur, Kanpur, India, KanGAL Tech. Rep. 2002008, 2002. [Online]. Available: http://www.iitk.ac.in/kangal/pub.htm

[65] K. Deb, L. Thiele, M. Laumanns, and E. Zizler, "Scalable multi-objective optimization test problems," in *Proc. IEEE CEC*, vol. 1. Honolulu, HI, USA, 2002, pp. 825–830.

[66] M. Emmerich, A. Deutz, J. Kruisselbrink, and P. K. Shukla, "Cone-based hypervolume indicators: Construction, properties, and efficient computation," in *Proc. EMO*, Sheffield, U.K., 2013, pp. 111–127.

[67] V. Khare, "Performance scaling of multi-objective evolutionary algorithms," School Comput. Sci., Univ. Birmingham, Birmingham, U.K., KanGal Tech. Rep. 2002009, 2002.

[68] G. Yen and Z. He, "Performance metric ensemble for multiobjective evolutionary algorithms," *IEEE Trans. Evol. Comput.*, vol. 18, no. 1, pp. 131–144, Feb. 2014.

[69] L. M. S. Russo and A. P. Francisco, "Quick hypervolume," *IEEE Trans. Evol. Comput.*, vol. 18, no. 4, pp. 481–502, Aug. 2014.

Chenwen Zhu was born in 1987. He received the B.E. degree in automation from Tongji University, Shanghai, China, in 2009, where he is currently working toward the Ph.D. degree with the Department of Control Science and Engineering.

From 2011 to 2013, he was a Visiting Researcher with the Genetic Algorithms Research and Applications Group and the Bio/computational Evolution in Action CONsortium Center for the Study of Evolution in Action, Michigan State University, East Lansing, MI, USA. He researched the application of multiobjective evolutionary algorithms in greenhouse micro-climate control. His research interests include intelligent control, multiobjective optimization, and evolutionary computation.

Lihong Xu (M'89) received the Ph.D. degree from the Department of Automatic Control, Southeast University, Nanjing, China, in 1991.

In 1994, he was a Professor with Southeast University. Since 1997, he has been a Professor with Tongji University, Shanghai, China. He is currently a Visiting Professor and an Advisor with the Greenhouse Research Team, Bio/computational Evolution in Action CONsortium, Forest Hill, MD, USA. His research interests include control theory, computational intelligence, and optimization theory.

Dr. Xu was a recipient of the first prize of the Science and Technology Advancement Award of the Ministry of Education of China, in 2005 and the second prize of the National Science and Technology Advancement Award of China, in 2007, respectively. He is a member of the ACM, and the President of the IEEE Computational Intelligence Society's Shanghai Chapter. He was the Co-Chair of the 2009 GEC Summit in Shanghai.

Erik D. Goodman received the B.S. degree in mathematics and the M.S. degree in system science from Michigan State University (MSU), East Lansing, MI, USA, and the Ph.D. degree in computer and communication sciences from University of Michigan, Ann Arbor, MI, USA, in 1972.

He is currently the Director of the Bio/computational Evolution in Action CONsortium Center for the Study of Evolution in Action, an National Science Foundation Science and Technology Center, MSU. Since 1984, he has been a Professor with the Department of Electrical and Computer Engineering, MSU, where he also co-directs the Genetic Algorithms Research and Applications Group. He is the Co-Founder in 1999 and the Former Vice President with the Technology of Red Cedar Technology, Inc., East Lansing, MI, USA. He is an Advisory Professor with Tongji University, Shanghai, China, and East China Normal University, Shanghai.

Dr. Goodman was the Chair of the Executive Board of International Society for Genetic and Evolutionary Computation from 2001 to 2004. From 2005 to 2007, he was the Founding Chair of the ACM SIG for Genetic and Evolutionary Computation. He is a Senior Fellow of the International Society for Genetic and Evolutionary Computation.